

Progress and Prospects In Magnetic Topological Materials

B. Andrei Bernevig¹, Claudia Felser², and Haim Beidenkopf³

¹ *Department of Physics, Princeton University, Princeton, New Jersey 08544, USA*

² *Max Plank Institute Chemical Physics of Solids, Dresden, Germany*

³ *Department of Condensed Matter Physics, Weizmann Institute of Science, Rehovot 7610001, Israel*

Magnetic topological materials represent a class of compounds whose properties are strongly influenced by the topology of the electronic wavefunctions coupled with the magnetic spin configuration. Such materials can support chiral electronic channels of perfect conduction, and can be used for an array of applications from information storage and control to dissipationless spin and charge transport. Here, we review the theoretical and experimental progress achieved in the field of magnetic topological materials beginning with the theoretical prediction of the Quantum Anomalous Hall Effect without Landau levels, and leading to the recent discoveries of magnetic Weyl semimetals and antiferromagnetic topological insulators. We outline the recent theoretical progress that resulted in the tabulation, for the first time, of all magnetic symmetry group representations and topology. We describe several experiments realizing Chern insulators, Weyl and Dirac magnetic semimetals, and an array of axionic and higher-order topological phases of matter as well as survey future perspectives.

I. INTRODUCTION

Topological insulators (TIs) and topological semimetals (TSMs), first predicted 15 years ago [1, 2], can exhibit robust boundary states, quantized bulk responses, and exotic transport properties. They represent a possible route towards manipulating quantum information [3], coherent spin transport [4], and high-efficiency catalysis [5]. Whereas a myriad of insulating and (semi)metallic non-magnetic topological phases have now been predicted, characterized and measured, magnetic materials have so far been scarce. These materials' interacting nature renders their theoretical prediction harder than that of their non-magnetic counterparts, yet they are experimentally attractive because magnetism potentially offers greater opportunity for manipulation of topological states. In the past 3 years, theoretical and experimental advances in topological magnetic materials have precipitated [6–11].

For background, in Box 1 we give an overview of the general steps needed for the high-throughput theoretical screening of magnetic topological materials (further technical details are available in Supplementary Information A). Once a candidate topological material has been synthesized (itself a challenge), a variety of experimental tools need to be marshalled to measure their electronic band structures as well as their transport properties and identify topological features: these are summarized in Box 2.

The main purpose of this Review is to discuss recent theoretical and experimental progress in this area using examples from each of the two main material classes – magnetic topological insulators and magnetic topological semimetals. Specifically, we will discuss the characteristic band structure features and transport phenomena of such systems based on two of the most well studied magnetic topological materials: the van der Waals antiferromagnetic MnBi_2Te_4 (a magnetic topological insulator) and the Kagome ferromagnetic Weyl $\text{Co}_3\text{Sn}_2\text{S}_2$ (a magnetic topological semimetal). Other magnetic topological possibilities exist that are

linked to orbital magnetism instead of spin magnetism; we will defer such discussion to the Supplementary Information B.

Finally, we will conclude with a brief discussion of the opportunities for further theoretical exploration and experimental discovery in this space, and what they might mean for both fundamental studies and practical applications.

II. THEORY OF MAGNETIC TOPOLOGICAL INSULATORS

The very first magnetic topological insulator is the (integer and fractional) quantum Hall effect, whose discovery and theoretical explanation resulted in two Nobel prizes, in 1985 and 1998. It was subsequently realized [12] by Haldane that an applied magnetic field is not necessary to realize a magnetic topological insulator, and research for the past 10 year theoretically uncovered other insulating phases of matter whose properties are defined by magnetic group topology.

The quantum anomalous Hall effect (QAHE) [12] has been realized by opening a magnetic mass gap (by either magnetic impurities [13, 14] or intrinsic magnetic order [10, 15, 16]) in the Dirac cone at the surface of a thin 3D TI film. This state is, however, the axion (higher order) insulator (AXI) with a chiral hinge mode, where the sample has been thinned to quasi-2D with magnetism added on the surface; it is not the original stoichiometric purely 2D Chern insulator CI [12]. The magnetic order mechanism in these samples is under debate (see [13, 17]), between RKKY (Mn-doped Bi_2Te_3 [18]) and Van Vleck [19] (Cr-doped $(\text{Bi},\text{Sb})_2\text{Te}_3$ [20]).

The 3D antiferromagnetic (AFM) TI [21, 22] is the only other magnetic TI that has been realized, in MnBi_2Te_4 [10] in Type-IV magnetic space group (MSG) $R_I\bar{3}c$ (No. 167.108) [23]. Fig[1] summarizes the different magnetic topological phases observed and predicted in MnBi_2Te_4 and related compounds. An AFM TI is the result of

turning on the AFM in a nonmagnetic time-reversal (TR)-invariant TI. Forcing doubling of the unit cell, the symmetry group becomes a combination ($\{T | 00\frac{1}{2}\}$) of TR (T) and half a lattice translation ($\{00\frac{1}{2}\}$). Before turning on the AFM, the strong TI exhibited a Dirac cone on each surface; the AFM gaps the Dirac cone on the surface perpendicular to the half lattice translation. On the side surfaces, the $\{T | 00\frac{1}{2}\}$ enforces Kramers degeneracy at $k_z = 0$ (but not at $k_z = \pi$). The Dirac node sits at $k_z = 0$ in the AFM Brillouin Zone (BZ), *irrespective* of its location (at $k_z = 0$ or π) in the larger non-magnetic BZ (see Fig. 1), as reported in [10].

Thin samples of $MnBi_2Te_4$ produce a QAHE expected to be more robust than that of magnetic-impurity doped TI [24–27]. When a Dirac fermion (exhibiting π Berry phase around the Fermi surface) is gapped, the resulting insulator has an integrated Berry curvature - Chern number - $C = 1/2$; the lower and upper surfaces can then either subtract (to lead to $C = 0$) or add, to lead to $C = 1$ QAHE. Whether they add or subtract depends on the surface exchange field. Even/odd number of non-magnetic unit cells will experience opposite/equal exchange field on the top and bottom surface, giving rise to $C = 0/1$. Furthermore, the application of a magnetic field can drive the magnetic moments ferromagnetically. Theoretically, FM $MnBi_2Te_4$ (with MSG $R\bar{3}m'$ (No. 166.101)) is a bulk Weyl semimetal (WSM) with one pair of Weyl points (WPs) along the $\Gamma - Z$ [26, 28]. In between the two WPs, in each k_z plane, the Chern number is 1 per k_z momentum. For a thin-film material of N layers, this momentum is quantized in units of $2\pi/N$, which, for N small, gaps the Weyl nodes due to quantum confinement. Hence the finite layer thin film of FM $MnBi_2Te_4$ can exhibit a QAHE with a Chern number greater than 1. In [29], a quantum confinement 5 meV gap is induced at the Γ point and $C = 2$.

The $C = 1$ QAHE state obtained by gapping a thin film of TI is a *static* AXI, a state of matter with the θ -angle (coefficient of the Chern-Simons form of the Berry potential $\vec{A}(\vec{k})$)

equal to π [30]. The discovery of higher order TIs (HOTIs) [31] resolved the link between the AXI and the QAHE. T symmetry breaking can drive a 3D TI into an AXI phase with gapped surface states and gapless (chiral) hinge modes [30, 32–38] which carry the Chern number of the QAHE. Inversion-symmetric TIs can be AXIs and at the same time magnetic HOTIs with *intrinsic* hinge states (see Fig. 1). [6, 7, 38–41]. Their bulk topology may be inferred from the Fu-Kane parity formula [32, 33, 42]; *all* of their surface states and Wilson loops are gapped. Gapless hinges provide chiral spectral flow [31, 43].

A large number of theoretically predicted but experimentally undiscovered topological states exist (see Fig.1). While the static AXI has been observed [10, 16, 44–46], it was predicted [47] that a *dynamical* mode of the AXI (phason as the dynamical mode) can arise from gapping *two* Weyl nodes spontaneously by charge-density wave (CDW) formation at the wave-vector between the nodes. This proposal remains unrealized, although its time-reversal counterpart (CDW in a non-centrosymmetric TR invariant Weyl) has been predicted and discovered in $(\text{TaSe}_4)_2\text{I}$ [48, 49]. In MSGs, AXI phases can be protected by other bulk symmetries such the product of twofold rotation and T [43, 50, 51] (see Fig.1). The magnetic *Möbius* TCIs [52, 53] host unpaired Dirac-cone surface states – like those of 3D TIs – appearing along surface glide lines and have been predicted in $\text{MnBi}_{2n}\text{Te}_{3n+1}$ [54–56] with canted magnetic moments. They are the T-breaking analogue of the hourglass topological crystalline insulators (TCI) [57, 58] [59] [60] in KHgSb. Glide mirror on some surfaces allows for a degeneracy along mirror symmetric lines in the BZ (see Fig.1).

In total, 4 different topological phases (3 of them shown in Fig.1 e) can be (theoretically) realized in the same compound formula, corresponding to different topological classifications: AFMTI (collinear AFM state), high-order Möbius insulator (in canted AFM state) and mirror TCI (in-plane FM), as well as a FM axion (out-of-plane FM) in $\text{MnBi}_8\text{Te}_{13}$, [61]. The difference in their topological classifications is a clear example of how different magnetic symmetry groups give rise to different topology.

Magnetic topological states implied by symmetry eigenvalues have recently been classified [7, 8], even though material predictions are scarce. Of these, spinful helical magnetic HOTI phases are related to rotational anomalies and exhibit trivial axion angles $\theta = 0(\text{mod } 2\pi)$. When terminated (see Fig.1) in nanorod geometries, the helical magnetic HOTIs generically exhibit even numbers of massless twofold surface Dirac cones (see Fig.1f) on surfaces perpendicular to a rotation axis similar to those in [62]. On their side-surfaces, domain walls between surfaces with oppositely-signed masses bind mirror-protected helical hinge states (Fig.1g).

III. MATERIALS FOR MAGNETIC TOPOLOGICAL INSULATORS

There are four main routes for turning a TI into a magnetic QAHE system, sketched in Fig.2: (a) extrinsic deposition of magnetic layers onto the surfaces of the TI, (b) doping the bulk TI with magnetic elements, (c) interleaving magnetic layers into the TI unit cell, (d) identifying intrinsic magnetically ordered TI states. The last two may introduce magnetic symmetries that directly affect the topological classification.

Several attempts made to fabricate hybrid heterostructures of magnetic over-layers on TI surfaces such as EuS over Bi_2Se_3 [63–69] have uncovered intriguing transport properties [70], but could not demonstrate quantized anomalous Hall conductance. An alternative path [13], inspired by semiconductor spintronics [71] is doping of the canonical TIs Bi_2Se_3 , Bi_2Te_3 or HgTe with magnetic ions (e.g. V, Mn, Cr, Sm) [13, 68, 72, 73], depicted in Fig.2b. In 2013, the QAHE was measured in thin films of Cr-doped $(\text{Bi}_{1-x}\text{Sb}_x)_2\text{Te}_3$ with a quantized Hall resistance ρ_{yx} observed up to temperatures of 30 mK [13]. In 2015 the QAHE was demonstrated in V doped $(\text{Bi}_{1-x}\text{Sb}_x)_2\text{Te}_3$ with a larger coercive field and in higher temperatures up to 100 mK [73]. While the transport experiments are quite promising, though limited to cryogenic temperatures, the spectroscopic investigation of the energy gap of the

corresponding surface states [46, 74–77] has so far been inconclusive. Low Curie temperatures, and the risk of inhomogeneous clustering of dopants thus gave way to intrinsic magnetic TIs.

Recently, a new family of intrinsic AFM TIs was discovered [10, 55, 56, 79] with the general composition $\text{MnTe}(\text{Bi}_2\text{Te}_3)_n$ (Fig.2e and f). MnBi_2Te_4 is the first member of the family with a Néel temperature T_N of 25 K [10]. MnBi_2Te_4 is a natural heterostructure of MnTe and Bi_2Te_3 [10]. The compound topology (band inversion) is akin to the Bi_2Te_3 quintuple layer, while the magnetism is related to MnTe . The combined symmetry of time reversal and half a unit cell translation protects the Dirac states parallel to the AFM order from gapping (Fig.2e) but gaps the surfaces perpendicular to it. Spectroscopic reports have been thus far inconclusive on the formation of a magnetic gap at the surface Dirac points: some ARPES measurements find a gapped surface spectrum [10, 80], other image gapless Dirac bands with weak response to lifting of the AFM order above the Neel temperature [81]. Local spectroscopic mappings in STM visualize high level of substitutional Mn atoms on Bi sites, posing a similar challenge to that encountered with magnetically doped TIs [82, 83]. Thin film quantization was shown to give rise to either a QAHE effect, [27] or an AXI [78] (Fig.2g and h, respectively). Accordingly, the $\text{MnTe}(\text{Bi}_2\text{Te}_3)_n$ family will undoubtedly open many new opportunities for magnetic WSMs, and beyond.

Meanwhile, an increasing number of intrinsic magnetic compounds (Fig.2d), are being identified and investigated in transport and spectroscopy in search of clear signatures of broken-TRS induced topology. These include the FM AHE Fe_3GeTe_2 [84], the AFM-TI EuCd_2As_2 and the AFM-TCI (and possibly a magnetic HOTI) EuIn_2As_2 , that we briefly discuss. Large anomalous Hall and Nernst signals were detected in the FM Fe_3GeTe_2 [84, 85], with T_c higher than room temperature in the few-layer limit of gated devices [86]. The anomalous Hall behavior is believed to originate from the intrinsic Berry curvature contribution due to gapping of a nodal line semimetallic state [84, 87]. No clear spectroscopic

evidence of topological states has been provided yet. EuCd₂As₂ is predicted [88, 89] to turn from a paramagnetic narrow gap semiconductor to AFM-TI below $T_N=10$ K with the easy axis perpendicular to the layers. The combined nonsymmorphic-TRS protects the Dirac surface states on the side surfaces that respect it, while the top and bottom facets are gapped forming a Chern or axion insulating states [88] that have been reported to exist by ARPES [90]. EuIn₂As₂ is predicted [89] to turn from a paramagnetic narrow gap semiconductor into a type-A AFM Axion insulator [91] or rather a magnetic HOTI [92] below $T_N=10$ K, neither of which is established spectroscopically [93]. A third classification arises when its AFM order aligns parallel to the layers and a magnetic mirror symmetry is restored, classifying the electronic phase as an AFM-TCI.

IV. THEORY OF MAGNETIC TOPOLOGICAL SEMIMETALS

More than 100 years ago Edwin Hall realized that all FM semimetals and metals exhibit an anomalously large Hall effect (AHE). Since the Hall resistivity versus an applied external magnetic field behaves similarly to the magnetization versus the external magnetic field, it was concluded that the AHE is proportional to the magnetization. Nowadays it is established that the Berry curvature plays an important role in determining the AHE in FM semimetals and metals [94]. Berry noted that an energy-level crossing leads to a physical band crossing that behaves as a magnetic monopole [95], the Weyl point. Magnetic WSMs are common: every crossing point in the band structure of a FM centro-symmetric compound is related to nodal lines or Weyl points.

The simplest topological semimetal, without time-reversal or crystalline symmetry is the solid-state realization of *conventional* Weyl fermions – twofold degeneracies appearing when two singly-degenerate bands cross, at any point in the BZ, and exhibiting linear dispersion away from the degeneracy point [96–98]. Weyl fermions carry a nontrivial topological invariant, the Chern number $|C| = 1$ evaluated on a sphere at energy E_F around the Weyl point.

This invariant renders Weyl nodes locally stable to gapping. The Berry curvature is concentrated near Weyl nodes giving a large AHE (angle) $\sigma_{\bar{W}} = \frac{e^2}{h} C \vec{1}_W$ in magnetic WSMs with Fermi level close to the Weyl nodes [98, 99], where $\vec{1}_W$ is the momentum vector between the two Weyl nodes. By the Mott relation $\alpha_{\bar{W}} = \left(\frac{\pi^3}{3}\right) \left(\frac{k_B T}{e}\right) d\sigma_{\bar{W}}(\epsilon) / d\epsilon_{\epsilon=E_F}$, the ANE is also expected to be large [100–103].

The \mathbb{Z} -valued Chern number of the Weyl points reflects the difference in the Chern number of 2D BZ planes above and below the Weyl point. Each BZ plane carrying nonzero Chern numbers projects on surfaces of the crystal to give rise to QH-like edge states, summing up into surface Fermi arcs spanning the momentum space between the projections of the bulk Weyl points. Higher-charge Weyl points appear when two or more Weyl nodes are pinned together by a crystalline rotation symmetry. The first prediction, still unrealized, of a $C = 2$ Weyl node, stabilized by C_4 symmetry, was in the FM phase of HgCr_2Se_4 [104] in the MSG *I41/am'd'* (No. 141.557) [23], in which strong AHE was reported [105].

A series of experimentally promising AFM TSM have been predicted [106–108] based on a search of large AHE in Mn_3X ($X=\text{Sn}$, Ge and Ir) and on direct ab-initio calculations [109] in Mn_3Sn and Mn_3Ge with Kagome layers Mn atoms (see section V 2). The non-collinear magnet Mn_3Sn in MSG *Cmc'm'* (No. 63.463) is a magnetic WSM candidate with 6 pairs of Weyl points. Under rigorous MTQC principles [6, 7], it was found that these Weyl points are "accidental": if the 6 Weyl points reported in [109] in half of the BZ were pairwise annihilated without closing a gap at the inversion-invariant momenta, the gapped phase would either be an axion insulator or a 3D QAH state.

CuMnAs and CuMnP have been proposed [110] to exhibit Dirac points. Their AFM order maintains the Type-III symmetry *IT* [23] leading to doubly degenerate bands at each $\mathbf{k} \in \text{BZ}$. Two pairs of these bands cross and their Dirac degenerate point is protected by a non-symmorphic $\{C_{2z}|_{\frac{1}{2},0,\frac{1}{2}}\}$. EuCd_2As_2 [89] was also proposed as a DSM in a Type-IV MSGs

$(D_{3d}^4 \oplus T'D_{3d}^4)$ [23]. Doubly degenerate bands exist due to $I\{T|0,0,\frac{1}{2}\}$ symmetry, and two pairs can cross with the Dirac point stabilized by C_{3v} symmetry. When three-fold rotation symmetry C_{3z} is broken, the DSM phase can evolve into the AFM TI phase. For magnetic nodal line semimetals were predicted in the layered system Fe_3GeTe_2 [87] without SOC. Similarly, in the FM Co_2MnGa [111] with space p group $Fm\bar{3}m$ (No. 225) [23], two majority spin bands near the Fermi level cross on the mirror planes stabilized by mirror symmetry. The nodal lines gap when the SOC is present, although in reality the SOC is negligible. Proposals of Nodal Line Semimetals NLSMs in FM phases of LaCl (LaBr) [112] have not been realized; we believe that most likely these materials are non-magnetic.

Nonmagnetic and magnetic symmetry groups allow 2, 3, 4, 6, and 8-fold degeneracy “new fermions” [113, 114] in the BZ. In (Type I [23]) space groups 3-, 4- and 6- dimensional degeneracies can appear; Type-III and Type-IV groups [23] support [113, 114] 8-fold double Dirac points [115] degeneracies. The chiral AFM phase of Mn_3IrSi is predicted [114] to host Spin-1 Weyl fermions with 3-fold degeneracies. Mn_3IrSi [114] and Nd_5Si_4 [6] are predicted to be chiral magnetic TSM. The 4, 6, and 8-fold new degeneracies are not protected by a Chern number (as in the case of WSM) and hence do not exhibit Fermi arcs on surfaces; they are novel Higher Order Semimetals (HOTSM) exhibiting *hinge* arcs [116]. A simple model for hinge arcs can be expressed as a k_z phase transition between a Quadrupole Insulator (QI) in [31] and a trivial insulator. Related arguments show that both Dirac HOTSMs and 6-fold degeneracies *universally* host intrinsic hinge states [116, 117].

v. MATERIALS FOR MAGNETIC TOPOLOGICAL SEMIMETALS

1. Ferromagnetic compounds

The FM WSM $\text{Co}_3\text{Sn}_2\text{S}_2$ in MSG $R\overline{3}m'$ (No. 166.101) has been extensively explored and characterized for its topological properties. Its crystal structure is composed of A-B stacked triangular layers of Sn and S and Kagome layers of magnetic Co ions (Fig.3, inset) captured in STM topography [9]. The compound hosts one electron more than the semiconducting non-magnetic Shandite $\text{Co}_3\text{InSnS}_2$. $\text{Co}_3\text{Sn}_2\text{S}_2$ fully polarized spin ($0.29\mu_B/\text{Co}$) leads to a half metallic FM with a relative high Curie temperature of 177 K with its spins oriented out of plane [119]. A single valence and conduction band cross the Fermi energy, leading to prediction of Weyl crossings, shown in Fig.3b. Experimental evidence for the bulk Weyl nodes close to the Fermi energy was provided by ARPES measurements (Fig.3c) [118], as well as confirmed by STM through quasi particle interference (Fig.3d).

Clear magneto-transport signatures of the magnetic topological state were reported prior to the spectroscopic verification. These include negative magneto-resistance under parallel current and magnetic field (Fig.3g), potentially signifying chiral anomaly, high anomalous Hall conductivity [119], and a significantly higher anomalous Nernst signal than conventional materials (Fig.3f) [120]. STM further finds presence of linearly dispersing step-edge modes (Fig.3g) [121], while theory predicts isolated Co_3Sn sheets will exhibit QAHE [123]. Furthermore, the Kagome structure of the magnetic Co ions can host flat band models due to the line-graph property of the lattice [124]. Intriguingly, a zero bias conductance peak has been detected in STM (Fig.3h) on the Co surface termination, with an unusual response to magnetic field [122, 125]. Bulk single crystals of $\text{Co}_3\text{Sn}_2\text{S}_2$ have been even used for a proof-of-concept investigations of the efficiency towards water oxidation [126].

All these suggest a new direction to search and synthesize magnetic TSMs in Kagome [109, 119, 127] and honeycomb-layer of a 3d-transition metal ions [128]. This family of materials exhibit Weyl and Dirac fermions in both FM and AFM materials. Examples to date include: FeSn [129], Fe_3Sn_2 [130], Mn_3Sn [131], Mn_3Ge [106, 132], and CoSn [133], as well as the $RMn_6\text{Sn}_6$ family with $R = \text{Tb}, \text{Gd}, \text{Tm}, \text{Lu}$ [134–136]. Experimental signatures include a

temperature independent enhanced AHE up to room temperature in Fe_3Sn_2 [130], and a gapped two-dimensional Dirac band close to the Fermi energy by ARPES. A giant spontaneous nematic energy shift, larger than any possible Zeeman splitting, hints at strong correlations in Fe_2Sn_3 [137]. To reduce the dimensionality and increase correlations effects, FeSn - with decoupled iron layers - was identified as an ideal Kagome lattice [129]. Flat bands and fully spin-polarized surface states (confirmed by ARPES) suggest the presence of spatially decoupled Kagome planes. For the summary of the anomalous transport properties of the Kagome compounds and the corresponding synthesis methods, please see Table I.

Another large family of half metallic Co_2 -Heusler compounds holds great potential as magnetic Weyl candidate materials because of their tunability. They were proposed in Co_2YZ ($Y = \text{V}, \text{Zr}, \text{Nb}, \text{Ti}, \text{Hf}$, $Z = \text{Si}, \text{Ge}, \text{Sn}$) [138] and Co_2MnZ ($Z = \text{Ga}, \text{Al}$) [139] and can be grown in bulk and thin films [140]. A leading magnetic topological semimetal candidate is Co_2MnGa that was verified spectroscopically in ARPES as a nodal line semimetal hosting drum head surface states [111]. Strong AHE indicating interplay between nodal lines and their partial gapping into Weyl points [141] close to the Fermi energy were reported in it and in Co_2MnAl [139]. The AHE in Co_2MnGa and Co_2MnAl is even larger than that magnetically induced in GdPtBi , leading to a Hall angle of 12 % [142] and 21 % [141], respectively. The synthesis methods, and the transport properties of GdPtBi and Co_2MnZ are summarized in Table I. Additionally, the large ANE signal is achievable at lower magnetic fields as it scales beyond the magnetization due to the Berry phase contribution. In Co_2MnGa an ANE with a remarkably high value SA_{yx} of $\sim 6.0 \mu_V K^{-1}$ at room temperature, (an order of magnitude higher than for conventional FMs), was reported [102, 143, 144]. High-throughput searches for large Berry phase contributions close to the Fermi energy have identified several magnetic compounds with the naturally abundant and low-cost element iron, such as the nodal line compounds Fe_3Ga and Fe_3Al [145]. The expected high efficiency of lateral thin film devices may pave the way for new large-area energy harvesting technology.

2. Antiferromagnetic compounds

The first magnetically induced WSM was realized in the AFM half Heusler compound GdPtBi [146]. GdPtBi and NdPtBi become WSMs only in applied fields of the order of 2 T [146–148]. Strong signatures typical for magnetic WSMs were observed in both compounds including the chiral anomaly, the gravitational anomaly, a large non-saturated negative quadratic magnetoresistance for fields of up to 60 T, an unusual intrinsic anomalous Hall effect, and planar Hall effect [146, 148–150]. In most AFM compounds the magnetic ordering is unknown, because large single crystals are needed for neutron scattering. Considering various AFM orders allows to construct a generalized Kane model with a resulting rich phase diagram ranging from Dirac, Weyl and nodal semimetal phases, type-B triple point phases, topological mirror (or glide), and AFM topological insulating phase [151]. The topological nature of Heusler half metallic compounds such as MnPtSb and MnPtBi, with a Curie temperature up to 1000 K [140], is still unexplored.

AFM order offers an even richer magnetic phase diagram than FM order. Collinear antiferromagnets with a zero net magnetic moment must have a net zero Berry curvature, although crossings can be sometimes observed in the band structure of an AFM metal. In agreement with this simplified picture the AHE is absent in nearly all AFMs that have zero magnetization. The three systems, hexagonal Mn₃Sn [131], Mn₃Ge [106, 132] and cubic Mn₃Ir [107] have non-collinear triangular AFM arrangements, which is the origin of a non-vanishing Berry curvature. Mn₃Sn and Mn₃Ge have Weyl points close to the Fermi energy, and show the predicted properties of an AHE even at room temperature [131, 132] and exhibit complex Fermi arcs in qualitative agreement with theory [131]. The chiral anomaly, was also reported in the anisotropic compound Mn₃Sn [152] as was a large ANE [153] and magneto

optical Kerr effect [154]. The strong response of the WSM compounds to external stimuli makes them promising candidates for topological AFM spintronics [155]. Another family of compounds exhibiting an intricate AFM order and showing promising experimental signatures in spectroscopy and magnetotransport, such as a singular angular magnetoresistance (SAMR), exceeding 1000% per radian, is $R\text{AlGe}$ with $R = \text{Ce}$ [156, 157], Pr [158] and the nonmagnetic La [159]. Lastly, we remark that the pyrochlore irridate family of materials, in which topological WSMs were first predicted [97], has remained largely unexplored. Their tetrahedral spin configuration gives rise to rich AFM orders [160] coupled to magnetic topological phases [161–163] as well as correlated AFM Mott states [164–166]. Remarkably, metallic modes [167] on AFM domain walls, thought to be a precursor of Fermi-arc states [168], were imaged within the otherwise Mott insulating state.

VI. FUTURE DIRECTIONS

Using high-throughput searches [6] a more systematic search for magnetic topological materials with high Curie temperatures, is important for quantum (computing/sensors) and classical (thermoelectrics/Hall sensors/efficient catalysts) applications. These following additional characteristics should be considered for material selection: (a) topological magnets with high Curie temperatures, which enable a high ANE signal close to room temperature; (b) low magnetic moment for eliminating stray magnetic fields in devices; or (c) hard magnets favorable for AHE and ANE at zero magnetic field; (d) low dimensional crystal structure and electronic structures for quantum confinement; and, finally, (e) frustrated atomic arrangement such as Kagome lattices for flat bands and non-collinear spin structures.

The design of a material that exhibits a high temperature QAHE via quantum confinement of a magnetic WSM, and its integration into quantum devices is desired. Indeed, several magnetic topological semimetals and insulators are predicted to realize QAHE in the thin film

limit [84, 123, 172]. The realization of the QAHE at room temperature would be revolutionary, overcoming the limitations of data-based technologies, which are affected by large electron scattering-induced power losses. This would pave the way to new generations of low energy consuming quantum electronic and spintronic devices.

Magnetic topological systems are a fertile field for further theoretical discoveries. While the complete stable topological indices of magnetic and nonmagnetic TIs, TCIs, and TSMs have been computed [6–8, 40, 173], the magnetic fragile topological indices remain an outstanding problem [174]. A classification of the magnetic obstructed atomic insulators - phases of matter described by bands which are not topological in the sense that they admit a localized Wannier description, but whose Wannier centers do not locate at the atom positions [175] – is still outstanding.

A further fundamental breakthrough would be the development of a framework to predict crossing points of WSM or DSM that are *very close* to the Fermi energy. The studying of topological materials displaying incommensurate magnetism is almost non-existent at the present time and should be pursued; it is unclear if in this case other topological classes besides the Chern QAHE class exists.

In parallel, the magnetic topological responses must also be developed. While for non-magnetic systems, we understand a series of responses such as chiral and gravitational anomaly, quantized photo-galvanic effects in Weyl, and topological defects we do not yet understand any *specific* responses that are unique to magnetic systems. A full classification of magnetic topological defects in crystalline TIs is absolutely necessary. Predictions of magneto-optical responses are needed, especially in the new, rotation-anomaly magnetic TIs. Predictions of *quantized* responses are particularly desired.

The field of magnetic topological superconductivity is also completely open. Since magnetic materials already have time-reversal breaking, they might exhibit topological excitations such as Majorana zero modes without the need for applying a magnetic field,

thereby rendering these systems useful for practical applications. While the types of phases that one obtains by proximitizing the surface of non-magnetic topological systems is mature, the similar studies for all the magnetic crystalline TIs are absent.

The next step is the theoretical introduction of bulk/surface interactions in topological materials. In the bulk, topological metals can give rise to many-body states by tuning interactions. The simplest example is a Weyl CDW axionic insulator, mirroring the non-magnetic experiment [48]. Many-body effects on the surface of magnetic TIs could give rise to topologically ordered states of matter.

ACKNOWLEDGMENT

B.A.B. work on magnetic topology is mainly supported by the DOE Grant No. DE-SC0016239. Further support comes from the Schmidt Fund for Innovative Research, Simons Investigator Grant No. 404513, the Packard Foundation, the Gordon and Betty Moore Foundation through Grant No. GBMF8685 towards the Princeton theory program, the NSF-EAGER No. DMR 1643312, NSF-MRSEC No. DMR-1420541 and DMR2011750, ONR No. N00014-20-1-2303, Gordon and Betty Moore Foundation through Grant GBMF8685 towards the Princeton theory program, BSF Israel US foundation No. 2018226, and the Princeton Global Network Funds. C. F. was supported by the ERC Advanced Grant No. 742068 ‘TOPMAT’ and by the Deutsche Forschungsgemeinschaft (DFG, German Research Foundation) under Germany’s Excellence Strategy through Würzburg-Dresden Cluster of Excellence on Complexity and Topology in Quantum Matter - ct.qmat (EXC 2147, project-id 390858490). B. A. B. received additional support from the Max Planck Society. Additional support was provided by the Gordon and Betty Moore Foundation through Grant GBMF8685 towards the Princeton theory program. H.B. acknowledges support from the European Research Council (ERC) under the European Union’s Horizon 2020 research and innovation

program (grant agreement no. 678702), and the German-Israeli Foundation (GIF, I-1364-303.7/2016).

REFERENCES

- [1] C. L. Kane and E. J. Mele, Quantum spin Hall effect in graphene, *Phys. Rev. Lett.* **95**, 226801 (2005).
- [2] B. A. Bernevig, T. L. Hughes, and S.-C. Zhang, Quantum spin Hall effect and topological phase transition in HgTe quantum wells, *Science* **314**, 1757 (2006).
- [3] A. Kitaev, Fault-tolerant quantum computation by anyons, *Annals of Physics* **303**, 2 (2003).

This paper shows the way to implement topological quantum computing in magnetic superconducting systems

- [4] D. Pesin and A. H. MacDonald, Spintronics and pseudospintronics in graphene and topological insulators, *Nature Materials* **11**, 409 (2012).
- [5] C. R. Rajamathi, U. Gupta, N. Kumar, H. Yang, Y. Sun, V. Sućić, C. Shekhar, M. Schmidt, H. Blumtritt, P. Werner, B. Yan, S. Parkin, C. Felser, and C. N. R. Rao, Weyl semimetals as hydrogen evolution catalysts, *Advanced Materials* **29**, 1606202 (2017).

This paper represents the first application of a Weyl semimetal for catalysis

- [6] Y. Xu, L. Elcoro, Z.-D. Song, B. J. Wieder, M. G. Vergniory, N. Regnault, Y. Chen, C. Felser, and B. A. Bernevig, High-throughput calculations of magnetic topological materials, *Nature* **586**, 702 (2020).

This paper represents the first high-throughput magnetic topological calculations.

- [7] L. Elcoro, B. J. Wieder, Z. Song, Y. Xu, B. Bradlyn, and B. A. Bernevig, Magnetic topological quantum chemistry (2020), arXiv:2010.00598 [cond-mat.mes-hall].

This paper develops the full theory of topological insulators and metals in magnetic groups

[8] H. Watanabe, H. C. Po, and A. Vishwanath, Structure and topology of band structures in the 1651 magnetic space groups, *Science Advances* **4**, 10.1126/sciadv.aat8685 (2018).

[9] N. Morali, R. Batabyal, P. K. Nag, E. Liu, Q. Xu, Y. Sun, B. Yan, C. Felser, N. Avraham, and H. Beidenkopf, Fermi-arc diversity on surface terminations of the magnetic Weyl semimetal $\text{Co}_3\text{Sn}_2\text{S}_2$, *Science* **365**, 1286 (2019), arXiv:1903.00509.

This paper shows the relevance of the distinct surface potentials imposed by three different terminations on the modification of the Fermi-arc contour and Weyl node connectivity.

[10] M. M. Otrokov, I. I. Klimovskikh, H. Bentmann, D. Estyunin, A. Zeugner, Z. S. Aliev, S. Gaß, A. U. B. Wolter, A. V. Koroleva, A. M. Shikin, M. Blanco-Rey, M. Hoffmann, I. P. Rusinov, A. Y. Vyazovskaya, S. V. Eremeev, Y. M. Koroteev, V. M. Kuznetsov, F. Freyse, J. Sañchez-Barriga, I. R. Amiraslanov, M. B. Babanly, N. T. Mamedov, N. A. Abdullayev, V. N. Zverev, A. Alfonsov, V. Kataev, B. Büchner, E. F. Schwier, S. Kumar, A. Kimura, L. Petaccia, G. Di Santo, R. C. Vidal, S. Schatz, K. Kißner, M. Unzelmann, C. H. Min, S. Moser, T. R. F. Peixoto, F. Reinert, A. Ernst, P. M. Echenique, A. Isaeva, and E. V. Chulkov, Prediction and observation of an antiferromagnetic topological insulator, *Nature* **576**, 416 (2019).

This paper predicts and realizes an antiferromagnetic topological insulator in a bulk material for the first time

[11] J. Noky, Y. Zhang, J. Goeth, C. Felser, and Y. Sun, Giant anomalous Hall and Nernst effect in magnetic cubic heusler compounds, *npj Comput Mater* **6**, 77 (2020).

This paper investigate systematically the Berry curvature of all magnetic Heusler compounds.

[12] F. D. M. Haldane, Model for a quantum Hall effect without landau levels: Condensed-matter realization of the "parity anomaly", *Phys. Rev. Lett.* **61**, 2015 (1988).

- [13] C.-Z. Chang, J. Zhang, X. Feng, J. Shen, Z. Zhang, M. Guo, K. Li, Y. Ou, P. Wei, L.-L. Wang, Z.-Q. Ji, Y. Feng, S. Ji, X. Chen, J. Jia, X. Dai, Z. Fang, S.-C. Zhang, K. He, Y. Wang, L. Lu, X.-C. Ma, Q.-K. Xu, Experimental Observation of the Quantum Anomalous Hall Effect in a Magnetic Topological Insulator *Science* **340**, 167 (2013).

This paper realizes the first model of a magnetic topological insulators (Chern Insulator)

- [14] J. G. Checkelsky, R. Yoshimi, A. Tsukazaki, K. S. Takahashi, Y. Kozuka, J. Falson, M. Kawasaki, and Y. Tokura, Trajectory of the anomalous Hall effect towards the quantized state in a ferromagnetic topological insulator, *Nature Physics* **10**, 731 (2014).

- [15] Y. Deng, Y. Yu, M. Z. Shi, Z. Guo, Z. Xu, J. Wang, X. H. Chen, and Y. Zhang, Quantum anomalous Hall effect in intrinsic magnetic topological insulator MnBi₂Te₄, *Science* **367**, 895 (2020).

- [16] Y. Gong, J. Guo, J. Li, K. Zhu, M. Liao, X. Liu, Q. Zhang, L. Gu, L. Tang, X. Feng, D. Zhang, W. Li, C. Song, L. Wang, P. Yu, X. Chen, Y. Wang, H. Yao, W. Duan, Y. Xu, S.-C. Zhang, X. Ma, Q.-K. Xue, and K. He, Experimental realization of an intrinsic magnetic topological insulator, *Chinese Physics Letters* **36**, 076801 (2019).

- [17] C.-Z. Chang and M. Li, Quantum anomalous Hall effect in time-reversal-symmetry breaking topological insulators, *Journal of Physics: Condensed Matter* **28**, 123002 (2016).

- [18] Y. S. Hor, P. Roushan, H. Beidenkopf, J. Seo, D. Qu, G. Checkelsky, L. A. Wray, D. Hsieh, Y. Xia, S.-Y. Xu, D. Qian, M. Z. Hasan, N. P. Ong, A. Yazdani, and R. J. Cava, Development of ferromagnetism in the doped topological insulator Bi_{2-x}Mn_xTe₃, *Phys. Rev. B* **81**, 195203 (2010).

- [19] R. Yu, W. Zhang, H.-J. Zhang, S.-C. Zhang, X. Dai, and Z. Fang, Quantized anomalous Hall effect in magnetic topological insulators, *Science* **329**, 61 (2010), <https://science.sciencemag.org/content/329/5987/61.full.pdf>.
- [20] C.-Z. Chang, J. Zhang, M. Liu, Z. Zhang, X. Feng, Li, L.-L. Wang, X. Chen, X. Dai, Z. Fang, X.-L. Qi, S.-C. Zhang, Y. Wang, K. He, X.-C. Ma, and Q.-K. Xue, Thin films of magnetically doped topological insulator with carrier-independent long-range ferromagnetic order, *Advanced Materials* **25**, 1065 (2013), <https://onlinelibrary.wiley.com/doi/10.1002/adma.201203493>.
- [21] R. S. K. Mong, A. M. Essin, and J. E. Moore, Antiferromagnetic topological insulators, *Phys. Rev. B* **81**, 245209 (2010).
- This paper writes down the first model of an antiferromagnetic topological insulator**
- [22] C. Fang, M. J. Gilbert, and B. A. Bernevig, Topological insulators with commensurate antiferromagnetism, *Phys. Rev. B* **88**, 085406 (2013).
- [23] C. Bradley and A. Cracknell, *The Mathematical Theory of Symmetry in Solids: Representation Theory for Point Groups and Space Groups* (Clarendon Press, 1972).
- [24] M. M. Otkrov, T. V. Menshchikova, M. G. Vergniory, I. P. Rusinov, A. Y. Vyazovskaya, Y. M. Koroteev, G. Bihlmayer, A. Ernst, P. M. Echenique, A. Arnau, and E. V. Chulkov, Highly-ordered wide bandgap materials for quantized anomalous Hall and magnetoelectric effects, *2D Materials* **4**, 025082 (2017).
- [25] M. M. Otkrov, I. P. Rusinov, M. Blanco-Rey, M. Hoffmann, A. Y. Vyazovskaya, S. V. Eremeev, A. Ernst, P. M. Echenique, A. Arnau, and E. V. Chulkov, Unique thickness-dependent properties of the van der Waals interlayer antiferromagnet MnBi₂Te₄ films, *Phys. Rev. Lett.* **122**, 107202 (2019).
- [26] J. Li, Y. Li, S. Du, Z. Wang, B.-L. Gu, S.-C. Zhang, K. He, W. Duan, and Y. Xu, Intrinsic magnetic topological insulators in van der Waals layered MnBi₂Te₄-family

materials, Science Advances 5, 10.1126/sciadv.aaw5685 (2019),

<https://advances.sciencemag.org/content/5/6/eaaw5685.full.pdf>.

- [27] Y. Deng, Y. Yu, M. Z. Shi, Z. Guo, Z. Xu, J. Wang, X. H. Chen, and Y. Zhang, Quantum anomalous Hall effect in intrinsic magnetic topological insulator MnBi₂Te₄, *Science* **367**, 895 (2020).
- [28] D. Zhang, M. Shi, T. Zhu, D. Xing, H. Zhang, and J. Wang, Topological axion states in the magnetic insulator MnBi₂Te₄ with the quantized magnetoelectric with the quantized magnetoelectric effect, *Phys. Rev. Lett.* **122**, 206401 (2019).
- [29] J. Ge, Y. Liu, J. Li, H. Li, T. Luo, Y. Wu, Y. Xu, and J. Wang, High-Chern-number and high-temperature quantum Hall effect without Landau levels, *National Science Review* **7**, 1280 (2020), <https://academic.oup.com/nsr/article-pdf/7/8/1280/33730346/nwaa089.pdf>.
- [30] X.-L. Qi, T. L. Hughes, and S.-C. Zhang, Topological field theory of time-reversal invariant insulators, *Phys. Rev. B* **78**, 195424 (2008).
- [31] W. A. Benalcazar, B. A. Bernevig, and T. L. Hughes, Quantized electric multipole insulators, *Science* **357**, 61 (2017).
- [32] T. L. Hughes, E. Prodan, and B. A. Bernevig, Inversionsymmetric topological insulators, *Phys. Rev. B* **83**, 245132 (2011).
- [33] A. M. Turner, Y. Zhang, R. S. K. Mong, and A. Vishwanath, Quantized response and topology of magnetic insulators with inversion symmetry, *Phys. Rev. B* **85**, 165120 (2012).
- [34] F. Zhang, C. L. Kane, and E. J. Mele, Surface state magnetization and chiral edge states on topological insulators, *Phys. Rev. Lett.* **110**, 046404 (2013).
- [35] L. Fu, C. L. Kane, and E. J. Mele, Topological insulators in three dimensions, *Phys. Rev. Lett.* **98**, 106803 (2007).

- [36] L. Fu and C. L. Kane, Topological insulators with inversion symmetry, *Phys. Rev. B* **76**, 045302 (2007).
- [37] S. Coh and D. Vanderbilt, Canonical magnetic insulators with isotropic magnetoelectric coupling, *Phys. Rev. B* **88**, 121106 (2013).
- [38] A. M. Essin, J. E. Moore, and D. Vanderbilt, Magnetoelectric polarizability and axion electrodynamics in crystalline insulators, *Phys. Rev. Lett.* **102**, 146805 (2009).
- [39] F. Schindler, A. M. Cook, M. G. Vergniory, Z. Wang, S. S. P. Parkin, B. A. Bernevig, and T. Neupert, Higher-order topological insulators, *Science Advances* **4**, 10.1126/sciadv.aat0346 (2018).
- [40] H. C. Po, A. Vishwanath, and H. Watanabe, Symmetrybased indicators of band topology in the 230 space groups, *Nature Communications* **8**, 50 (2017).
- [41] Z. Wang, B. J. Wieder, J. Li, B. Yan, and B. A. Bernevig, Higher-order topology, monopole nodal lines, and the origin of large fermi arcs in transition metal dichalcogenides $X\text{Te}_2$ ($X = \text{Mo}, \text{W}$), *Phys. Rev. Lett.* **123**, 186401 (2019).
- [42] A. M. Turner, Y. Zhang, and A. Vishwanath, Entanglement and inversion symmetry in topological insulators, *Phys. Rev. B* **82**, 241102 (2010).
- [43] B. J. Wieder and B. A. Bernevig, The Axion Insulator as a Pump of Fragile Topology, ArXiv e-prints (2018), [arXiv:1810.02373](https://arxiv.org/abs/1810.02373).
- [44] M. Mogi, M. Kawamura, R. Yoshimi, A. Tsukazaki, Kozuka, N. Shirakawa, K. A.⁺ S. Takahashi, M. Kawasaki, and Y. Tokura, A magnetic heterostructure of topological insulators as a candidate for an axion insulator, *Nature Materials* **16**, 516 (2017).

This paper has realized the first step towards the realization of an axion insulator by engineered heterostructures with modulation-doped TI films

- [45] D. Xiao, J. Jiang, J.-H. Shin, W. Wang, F. Wang, Y.-F. Zhao, C. Liu, W. Wu, M. H. W. Chan, N. Samarth, and C.-Z. Chang, Realization of the axion insulator state in quantum anomalous Hall sandwich heterostructures, *Phys. Rev. Lett.* **120**, 056801 (2018).

[46] S.-Y. Xu, M. Neupane, C. Liu, D. Zhang, A. Richardella, L. Andrew Wray, N. Alidoust, M. Leandersson, T. Balasubramanian, J. Sanchez-Barriga, O. Rader, G. Landolt, B. Slomski, J. Hugo Dil, J. Osterwalder, T.-R. Chang, H.-T. Jeng, H. Lin, A. Bansil, N. Samarth, and M. Zahid Hasan, Hedgehog spin texture and Berry’s phase tuning in a magnetic topological insulator, *Nature Physics* **8**, 616 (2012).

[47] Z. Wang and S.-C. Zhang, Chiral anomaly, charge density waves, and axion strings from Weyl semimetals, *Phys. Rev. B* **87**, 161107 (2013).

[48] J. Gooth, B. Bradlyn, S. Honnali, C. Schindler, N. Kumar, J. Noky, Y. Qi, C. Shekhar, Y. Sun, Z. Wang, B. A. Bernevig, and C. Felser, Axionic charge-density wave in the Weyl semimetal $(\text{TaSe}_4)_2\text{I}$, *Nature* **575**, 315 (2019).

First realization of an axion quasiparticle in a charge density wave Weyl semimetal.

[49] W. Shi, B. J. Wieder, H. L. Meyerheim, Y. Sun, Zhang, Y. Li, L. Shen, Y. Qi, L. Yang, J. Jena, P. Werner, K. Koepernik, S. Parkin, Y. Chen, C. Felser, B. A. Bernevig, and Z. Wang, A charge-density-wave topological semimetal, *Nature Physics* **17**, 381 (2021).

[50] J. Ahn and B.-J. Yang, Symmetry representation approach to topological invariants in $C_{2z}t$ -symmetric systems, *Phys. Rev. B* **99**, 235125 (2019).

[51] N. Varnava, I. Souza, and D. Vanderbilt, Axion coupling in the hybrid wannier representation, *Phys. Rev. B* **101**, 155130 (2020).

[52] K. Shiozaki, M. Sato, and K. Gomi, Topological crystalline materials: General formulation, module structure, and wallpaper groups, *Phys. Rev. B* **95**, 235425 (2017).

[53] C. Fang and L. Fu, New classes of three-dimensional topological crystalline insulators: Nonsymmorphic and magnetic, *Phys. Rev. B* **91**, 161105 (2015).

This paper realizes the first models of rotational anomaly topological insulators

[54] R.-X. Zhang, F. Wu, and S. Das Sarma, Mobius insulator and higher-order topology in $\text{MnBi}_{2n}\text{Te}_{3n+1}$, *Phys. Rev. Lett.* **124**, 136407 (2020).

This paper predicts several topological phases in the MnBiTe family

- [55] Z. S. Aliev, I. R. Amiraslanov, D. I. Nasonova, A. V. Shevelkov, N. A. Abdullayev, Z. A. Jahangirli, E. N. Orujlu, M. M. Otrokov, N. T. Mamedov, M. B. Babanly, and E. V. Chulkov, Novel ternary layered manganese bismuth tellurides of the MnTe-Bi₂Te₃ system: Synthesis and crystal structure, *Journal of Alloys and Compounds* **789**, 443 (2019).
- [56] I. I. Klimovskikh, M. M. Otrokov, D. Estyunin, S. V. Eremeev, S. O. Filnov, A. Koroleva, E. Shevchenko, V. Voroshnin, I. P. Rusinov, M. Blanco-Rey, M. Hoffmann, Z. S. Aliev, M. B. Babanly, I. R. Amiraslanov, N. A. Abdullayev, V. N. Zverev, A. Kimura, O. E. Tereshchenko, K. A. Kokh, L. Petaccia, G. Di Santo, A. Ernst, P. M. Echenique, N. T. Mamedov, A. M. Shikin, and E. V. Chulkov, Variety of magnetic topological phases in the (MnBi₂Te₄)(Bi₂Te₃)_m family, *npj Quantum Mater.* **12**, 20 (2019).
- [57] Z. Wang, A. Alexandradinata, R. J. Cava, and B. A. Bernevig, Hourglass fermions, *Nature* **532**, 189 (2016).
- [58] B. J. Wieder, B. Bradlyn, Z. Wang, J. Cano, Y. Kim, H.-S. D. Kim, A. M. Rappe, C. L. Kane, and B. A. Bernevig, Wallpaper fermions and the nonsymmorphic Dirac insulator, *Science* **361**, 246 (2018).
- [59] J. Ma, C. Yi, B. Lv, Z. Wang, S. Nie, L. Wang, L. Kong, Y. Huang, P. Richard, P. Zhang, K. Yaji, K. Kuroda, S. Shin, H. Weng, B. A. Bernevig, Y. Shi, T. Qian, and H. Ding, Experimental evidence of hourglass fermion in the candidate nonsymmorphic topological insulator KHgSb, *Science Advances* **3**, e1602415 (2017).
- [60] S. Liang, S. Kushwaha, T. Gao, M. Hirschberger, J. Li, Z. Wang, K. Stolze, B. Skinner, B. A. Bernevig, R. J. Cava, and N. P. Ong, A gap-protected zero-Hall effect state in the quantum limit of the non-symmorphic metal KHgSb, *Nature Materials* **18**, 443 (2019).

- [61] C. Hu, L. Ding, K. N. Gordon, B. Ghosh, H.-J. Tien, H. Li, A. G. Linn, S.-W. Lien, C.-Y. Huang, S. Mackey, J. Liu, P. V. S. Reddy, B. Singh, A. Agarwal, A. Bansil, M. Song, D. Li, S.-Y. Xu, H. Lin, H. Cao, T.-R. Chang, D. Dessau, and N. Ni, Realization of an intrinsic ferromagnetic topological state in MnBi₈Te₁₃, *Science Advances* **6**, eaba4275 (2020).
- [62] C. Fang and L. Fu, New classes of topological crystalline insulators having surface rotation anomaly, *Science Advances* **5**, eaat2374 (2019).
- [63] P. Wei, F. Katmis, B. A. Assaf, H. Steinberg, P. JarilloHerrero, D. Heiman, and J. S. Moodera, Exchangecoupling-induced symmetry breaking in topological insulators, *Phys. Rev. Lett.* **110**, 186807 (2013).
- [64] F. Katmis, V. Lauter, F. S. Nogueira, B. A. Assaf, M. E. Jamer, P. Wei, B. Satpati, J. W. Freeland, I. Eremin, D. Heiman, P. Jarillo-Herrero, and J. S. Moodera, A high-temperature ferromagnetic topological insulating phase by proximity coupling, *Nature* **533**, 513 (2016).
- [65] M. Lang, M. Montazeri, M. C. Onbasli, X. Kou, Y. Fan, P. Upadhyaya, K. Yao, F. Liu, Y. Jiang, W. Jiang, K. L. Wong, G. Yu, J. Tang, T. Nie, L. He, R. N. Schwartz, Y. Wang, C. A. Ross, and K. L. Wang, Proximity induced high-temperature magnetic order in topological insulator - Ferrimagnetic insulator heterostructure, *Nano Letters* **14**, 3459 (2014).
- [66] S. Tang, C. Zhang, D. Wong, Z. Pedramrazi, H. Z. Tsai, C. Jia, B. Moritz, M. Claassen, H. Ryu, S. Kahn, J. Jiang, H. Yan, M. Hashimoto, D. Lu, R. G. Moore, C. C. Hwang, C. Hwang, Z. Hussain, Y. Chen, M. M. Ugeda, Z. Liu, X. Xie, T. P. Devereaux, M. F. Crommie, S. K. Mo, and Z. X. Shen, Quantum spin Hall state in monolayer 1T'-WTe₂, *Nature Physics* **13**, 683 (2017) .
- [67] T. Hirahara, S. V. Eremeev, T. Shirasawa, Y. Okuyama, T. Kubo, R. Nakanishi, R. Akiyama, A. Takayama, T. Hajiri, S. I. Ideta, M. Matsunami, K. Sumida, K. Miyamoto,

Y. Takagi, K. Tanaka, T. Okuda, T. Yokoyama, S. I. Kimura, S. Hasegawa, and E. V. Chulkov, Large-Gap Magnetic Topological Heterostructure Formed by Subsurface Incorporation of a Ferromagnetic Layer, *Nano Letters* **17**, 3493 (2017).

- [68] T. Hirahara, M. M. Otrokov, T. T. Sasaki, K. Sumida, Y. Tomohiro, S. Kusaka, Y. Okuyama, S. Ichinokura, M. Kobayashi, Y. Takeda, K. Amemiya, T. Shirasawa, S. Ideta, K. Miyamoto, K. Tanaka, S. Kuroda, T. Okuda, K. Hono, S. V. Eremeev, and E. V. Chulkov, Fabrication of a novel magnetic topological heterostructure and temperature evolution of its massive Dirac cone, *Nature Communications* **11**, 1 (2020).
- [69] J. A. Krieger, C. Z. Chang, M. A. Husanu, D. Sostina, Ernst, M. M. Otrokov, T. Prokscha, T. Schmitt, A. Suter, M. G. Vergniory, E. V. Chulkov, J. S. Moodera, V. N. Strocov, and Z. Salman, Spectroscopic perspective on the interplay between electronic and magnetic properties of magnetically doped topological insulators, *Physical Review B* **96**, 184402 (2017), arXiv:1710.06238.
- [70] L. D. Alegria, H. Ji, N. Yao, J. J. Clarke, R. J. Cava, and J. R. Petta, Large anomalous Hall effect in ferromagnetic insulator-topological insulator heterostructures, *Appl. Phys. Lett* **105**, 053512 (2014).
- [71] S. Wolf, D. De, R. Buhrman, J. Daughton, S. von Molnar, M. Roukes, A. Chtchelkanova, and D. Treger, Spintronics: A spin-based electronics vision for the future, *SCIENCE* **294**, 1488 (2001).
- [72] Y. Tokura, K. Yasuda, and A. Tsukazaki, Magnetic topological insulators, *Nature Reviews Physics*, **1**, 126 (2019).

This paper reviews the basic concepts of magnetic topological insulators, their experimental realization and the verification of their emergent properties

- [73] C.-Z. Chang, W. Zhao, D. Y. Kim, H. Zhang, B. A. Assaf, D. Heiman, S.-C. Zhang, C. Liu, M. H. W. Chan, and J. S. Moodera, High-precision realization of robust quantum

anomalous Hall state in a hard ferromagnetic topological insulator, **NATURE MATERIALS** **14**, 473 (2015).

- [74] Y. L. Chen, J. H. Chu, J. G. Analytis, Z. K. Liu, K. Igarashi, H. H. Kuo, X. L. Qi, S. K. Mo, R. G. Moore, D. H. Lu, M. Hashimoto, T. Sasagawa, S. C. Zhang, I. R. Fisher, Z. Hussain, and Z. X. Shen, Massive Dirac Fermion on the Surface of a Magnetically Doped Topological Insulator, **Science** **329**, 659 (2010) .
- [75] E. O. Lachman, A. F. Young, A. Richardella, J. Cuppens, H. R. Naren, Y. Anahory, A. Y. Meltzer, A. Kandala, S. Kempinger, Y. Myasoedov, M. E. Huber, N. Samarth, and E. Zeldov, Visualization of superparamagnetic dynamics in magnetic topological insulators, **Science Advances** **1**, e1500740 (2015) .
- [76] H. Beidenkopf, P. Roushan, J. Seo, L. Gorman, I. Drozdov, Y. S. Hor, R. J. Cava, and A. Yazdani, Spatial fluctuations of helical Dirac fermions on the surface of topological insulators, **Nature Physics** **7**, 939 (2011) .
- [77] Lee, C. K. Kim, J. Lee, S. J. L. Billinge, R. Zhong, A. Schneeloch, T. Liu, T. Valla, J. M. Tranquada, G. Gu, and J. C. S. Davis, Imaging Dirac-mass disorder from magnetic dopant atoms in the ferromagnetic topological insulator $\text{Cr}_x(\text{Bi}_{0.1}\text{Sb}_{0.9})_{2-x}\text{Te}_3$, **Proceedings of the National Academy of Sciences** **112**, 1316 (2015),.
- [78] C. Liu, Y. Wang, H. Li, Y. Wu, Y. Li, J. Li, K. He, Y. Xu, J. Zhang, and Y. Wang, Robust axion insulator and Chern insulator phases in a two-dimensional antiferromagnetic topological insulator, **Nature Materials** **19**, 522 (2020).
- [79] E. D. L. Rienks, S. Wimmer, J. Sánchez-Barriga, O. Caha, P. S. Mandal, J. Růžička, A. Ney, H. Steiner, V. V. Volobuev, H. Groiss, M. Albu, G. Kothleitner, J. Michalička, S. A. Khan, J. Minár, H. Ebert, G. Bauer, F. Freyse, A. Varykhalov, O. Rader, and G. Springholz, Large magnetic gap at the Dirac point in $\text{Bi}_2\text{Te}_3/\text{MnBi}_2\text{Te}_4$ heterostructures, **Nature** **576**, 423 (2019).

- [80] S. H. Lee, Y. Zhu, Y. Wang, L. Miao, T. Pillsbury, H. Yi, S. Kempinger, J. Hu, C. A. Heikes, P. Quarterman, W. Ratcliff, J. A. Borchers, H. Zhang, X. Ke, D. Graf, N. Alem, C.-Z. Chang, N. Samarth, and Z. Mao, Spin scattering and noncollinear spin structureinduced intrinsic anomalous Hall effect in antiferromagnetic topological insulator MnBi_2Te_4 , *Physical Review Research* **1**, 012011(R) (2019) .
- [81] H. Li, S.-Y. Gao, S.-F. Duan, Y.-F. Xu, K.-J. Zhu, S.-J. Tian, J.-C. Gao, W.-H. Fan, Z.-C. Rao, J.-R. Huang, J.-J. Li, D.-Y. Yan, Z.-T. Liu, W.-L. Liu, Y.-B. Huang, Y.-L. Li, Y. Liu, G.-B. Zhang, P. Zhang, T. Kondo, S. Shin, H.-C. Lei, Y.-G. Shi, W.-T. Zhang, H.-M. Weng, T. Qian, and H. Ding, Dirac Surface States in Intrinsic Magnetic Topological Insulators EuSn_2As_2 and $\text{MnBi}_{2n}\text{Te}_{3n+1}$, *Physical Review X* **9**, 041039 (2019) .
- [82] J. Q. Yan, Q. Zhang, T. Heitmann, Z. Huang, K. Y. Chen, J. G. Cheng, W. Wu, D. Vaknin, B. C. Sales, and R. J. McQueeney, Crystal growth and magnetic structure of MnBi_2Te_4 , *Physical Review Materials* **3**, 064202 (2019) .
- [83] Y. Yuan, X. Wang, H. Li, J. Li, Y. Ji, Z. Hao, Y. Wu, K. He, Y. Wang, Y. Xu, W. Duan, W. Li, and Q.K. Xue, Electronic States and Magnetic Response of MnBi_2Te_4 by Scanning Tunneling Microscopy and Spectroscopy, *Nano Lett.* **20**, 3271 (2020).
- [84] X. Lin and J. Ni, Layer-dependent intrinsic anomalous Hall effect in Fe_3GeTe_2 , *Phys. Rev. B* **100**, 085403 (2019).
- [85] J. Xu, W. A. Phelan, and C.-L. Chien, Large Anomalous Nernst Effect in a van der Waals Ferromagnet Fe_3GeTe_2 , *Nano Letters* **19**, 8250 (2019).
- [86] Y. Deng, Y. Yu, Y. Song, J. Zhang, N. Z. Wang, Z. Sun, Y. Yi, Y. Z. Wu, S. Wu, J. Zhu, J. Wang, X. H. Chen, and Y. Zhang, Gate-tunable room-temperature ferromagnetism in two-dimensional Fe_3GeTe_2 , *Nature* **563**, 94 (2018), arXiv:1803.02038.

- [87] K. Kim, J. Seo, E. Lee, K. T. Ko, B. S. Kim, B. G. Jang, M. Ok, J. Lee, Y. J. Jo, W. Kang, J. H. Shim, C. Kim, H. W. Yeom, B. Il Min, B. J. Yang, and J. S. Kim, Large anomalous Hall current induced by topological nodal lines in a ferromagnetic van der Waals semimetal, *Nature Materials* **17**, 794 (2018).
- [88] L.-L. Wang, N. H. Jo, B. Kuthanazhi, Y. Wu, R. J. McQueeney, A. Kaminski, and P. C. Canfield, Single pair of weyl fermions in the half-metallic semimetal EuCd₂As₂, *Phys. Rev. B* **99**, 245147 (2019).
- [89] G. Hua, S. Nie, Z. Song, R. Yu, G. Xu, and K. Yao, Dirac semimetal in type-IV magnetic space groups, *Phys. Rev. B* **98**, 201116 (2018).
- [90] J. Ma, H. Wang, S. Nie, C. Yi, Y. Xu, H. Li, J. Jandke, W. Wulfhekel, Y. Huang, D. West, P. Richard, A. Chikina, V. N. Strocov, J. Mesot, H. Weng, S. Zhang, Y. Shi, T. Qian, M. Shi, and H. Ding, Emergence of Nontrivial Low-Energy Dirac Fermions in Antiferromagnetic EuCd₂As₂, *Advanced Materials* **32**, 1907565 (2020).
- [91] Y. Xu, Z. Song, Z. Wang, H. Weng, and X. Dai, Higher-Order Topology of the Axion Insulator EuIn₂As₂, *Physical Review Letters* **122**, 256402 (2019), arXiv:1903.09856.
- [92] X. Gui, I. Pletikosic, H. Cao, H. J. Tien, X. Xu, R. Zhong, G. Wang, T. R. Chang, S. Jia, T. Valla, W. Xie, and R. J. Cava, A New Magnetic Topological Quantum Material Candidate by Design, *ACS Central Science* **5**, 900 (2019), arXiv:1903.03888.
- [93] T. Sato, Z. Wang, D. Takane, S. Souma, C. Cui, Y. Li, K. Nakayama, T. Kawakami, Y. Kubota, C. Cacho, T. K. Kim, A. Arab, V. N. Strocov, Y. Yao, and T. Takahashi, Signature of band inversion in the antiferromagnetic phase of axion insulator candidate euin₂as₂, *Phys. Rev. Research* **2**, 033342 (2020).
- [94] N. Nagaosa, J. Sinova, S. Onoda, A. H. MacDonald, and N. P. Ong, Anomalous Hall effect, *Rev. Mod. Phys.* **82**, 1539 (2010).
- [95] M. V. Berry, Quantal phase factors accompanying adiabatic changes, *Proceedings of the Royal Society of London. A. Mathematical and Physical Sciences* **392**, 45 (1984).

- [96] S. Murakami, Phase transition between the quantum spin Hall and insulator phases in 3d: emergence of a topological gapless phase, *New Journal of Physics* **9**, 356 (2007).
- [97] X. Wan, A. M. Turner, A. Vishwanath, and S. Y. Savrasov, Topological semimetal and fermi-arc surface states in the electronic structure of pyrochlore iridates, *Phys. Rev. B* **83**, 205101 (2011).
- [98] A. A. Burkov and L. Balents, Weyl semimetal in a topological insulator multilayer, *Phys. Rev. Lett.* **107**, 127205 (2011).
- [99] K.-Y. Yang, Y.-M. Lu, and Y. Ran, Quantum Hall effects in a weyl semimetal: Possible application in pyrochlore iridates, *Phys. Rev. B* **84**, 075129 (2011).
- [100] X. Li, L. Xu, L. Ding, J. Wang, M. Shen, X. Lu, Z. Zhu, and K. Behnia, Anomalous Nernst and Righi-Leduc effects in Mn₃Sn: Berry curvature and entropy flow, *Phys. Rev. Lett.* **119**, 056601 (2017).
- [101] G. Sharma, P. Goswami, and S. Tewari, Nernst and magnetothermal conductivity in a lattice model of Weyl fermions, *Phys. Rev. B* **93**, 035116 (2016).
- [102] A. Sakai, Y. P. Mizuta, A. A. Nugroho, R. Sihombing, T. Koretsune, M.-T. Suzuki, N. Takemori, R. Ishii, D. Nishio-Hamane, R. Arita, P. Goswami, and S. Nakatsuji, Giant anomalous Nernst effect and quantumcritical scaling in a ferromagnetic semimetal, *Nature Physics* **14**, 1119 (2018).
- [103] J. Noky, J. Gayles, C. Felser, and Y. Sun, Strong anomalous Nernst effect in collinear magnetic Weyl semimetals without net magnetic moments, *Phys. Rev. B* **97**, 220405 (2018).
- [104] C. Fang, M. J. Gilbert, X. Dai, and B. A. Bernevig, Multi-weyl topological semimetals stabilized by point group symmetry, *Phys. Rev. Lett.* **108**, 266802 (2012).
- [105] N. I. Solin and N. M. Chebotaev, Magnetoresistance and Hall effect of the magnetic semiconductor HgCr₂Se₄ in strong magnetic fields, *Physics of the Solid State* **39**, 754 (1997).

- [106] J. Kübler and C. Felser, Non-collinear antiferromagnets and the anomalous Hall effect, *EPL (Europhysics Letters)* **108**, 67001 (2014).
- [107] H. Chen, Q. Niu, and A. H. MacDonald, Anomalous Hall effect arising from noncollinear antiferromagnetism, *Phys. Rev. Lett.* **112**, 017205 (2014).
- [108] Y. Zhang, Y. Sun, H. Yang, J. Železný, S. P. P. Parkin, C. Felser, and B. Yan, Strong anisotropic anomalous Hall effect and spin Hall effect in the chiral antiferromagnetic compounds Mn_3X ($X = Ge, Sn, Ga, Ir, Rh$, and Pt), *Phys. Rev. B* **95**, 075128 (2017).
- [109] H. Yang, Y. Sun, Y. Zhang, W.-J. Shi, S. S. P. Parkin, and B. Yan, Topological Weyl semimetals in the chiral antiferromagnetic materials Mn_3Ge and Mn_3Sn , *New Journal of Physics* **19**, 015008 (2017).
- [110] P. Tang, Q. Zhou, G. Xu, and S.-C. Zhang, Dirac fermions in an antiferromagnetic semimetal, *Nature Physics* **12**, 1100 (2016).
- [111] I. Belopolski, K. Manna, D. S. Sanchez, G. Chang, B. Ernst, J. Yin, S. S. Zhang, T. Cochran, N. Shumiya, H. Zheng, B. Singh, G. Bian, D. Multer, M. Litskevich, X. Zhou, S.-M. Huang, B. Wang, T.-R. Chang, S.-Y. Xu, A. Bansil, C. Felser, H. Lin, and M. Z. Hasan, Discovery of topological Weyl fermion lines and drumhead surface states in a room temperature magnet, *Science* **365**, 1278 (2019).
- [112] S. Nie, H. Weng, and F. B. Prinz, Topological nodal-line semimetals in ferromagnetic rare-earth-metal monohalides, *Phys. Rev. B* **99**, 035125 (2019).
- [113] B. Bradlyn, J. Cano, Z. Wang, M. G. Vergniory, C. Felser, R. J. Cava, and B. A. Bernevig, Beyond Dirac and Weyl fermions: Unconventional quasiparticles in conventional crystals, *Science* **353**, 558 (2016).
- [114] J. Cano, B. Bradlyn, and M. G. Vergniory, Multifold nodal points in magnetic materials, *APL Materials* **7**, 101125 (2019).
- [115] B. J. Wieder, Y. Kim, A. M. Rappe, and C. L. Kane, Double dirac semimetals in three dimensions, *Phys. Rev. Lett.* **116**, 186402 (2016).

- [116] B. J. Wieder, Z. Wang, J. Cano, X. Dai, L. M. Schoop, B. Bradlyn, and B. A. Bernevig, Strong and fragile topological dirac semimetals with higher-order fermi arcs, *Nature Communications* **11**, 627 (2020).
- [117] M. Lin and T. L. Hughes, Topological quadrupolar semimetals, *Phys. Rev. B* **98**, 241103 (2018).
- [118] D. F. Liu, A. J. Liang, E. K. Liu, Q. N. Xu, Y. W. Li, C. Chen, D. Pei, W. J. Shi, S. K. Mo, P. Dudin, T. Kim, C. Cacho, G. Li, Y. Sun, L. X. Yang, Z. K. Liu, S. S. P. Parkin, C. Felser, and Y. L. Chen, Magnetic Weyl semimetal phase in a Kagomé crystal, *Science* **365**, 1282 (2019).
- [119] E. Liu, Y. Sun, N. Kumar, L. Muechler, A. Sun, L. Jiao, S.-Y. Yang, D. Liu, A. Liang, Q. Xu, J. Kroder, V. Süß, H. Borrmann, C. Shekhar, Z. Wang, C. Xi, W. Wang, W. Schnelle, S. Wirth, Y. Chen, S. T. B. Goennenwein, and C. Felser, Giant anomalous Hall effect in a ferromagnetic Kagome-lattice semimetal, *Nature Physics* **14**, 1125 (2018).
- [120] S. N. Guin, P. Vir, Y. Zhang, N. Kumar, S. J. Watzman, C. Fu, E. Liu, K. Manna, W. Schnelle, J. Gooth, C. Shekhar, Y. Sun, and C. Felser, Zero-Field Nernst Effect in a Ferromagnetic Kagome-Lattice Weyl Semimetal $\text{Co}_3\text{Sn}_2\text{S}_2$, *Advanced Materials* **31**, 1 (2019).
- [121] S. Howard, L. Jiao, Z. Wang, Noam Morali, R. Batabyal, P. Kumar-Nag, N. Avraham, H. Beidenkopf, P. Vir, E. Liu, C. Shekhar, C. Felser, T. Hughes, and V. Madhavan, Evidence for one-dimensional chiral edge states in a magnetic Weyl semimetal $\text{Co}_3\text{Sn}_2\text{S}_2$, *Nature Communications* **12**, 4269 (2021).
- [122] Y. Xu, J. Zhao, C. Yi, Q. Wang, Q. Yin, Y. Wang, X. Hu, L. Wang, E. Liu, G. Xu, L. Lu, A. A. Soluyanov, H. Lei, Y. Shi, J. Luo, and Z.-G. Chen, Electronic correlations and flattened band in magnetic Weyl semimetal $\text{Co}_3\text{Sn}_2\text{S}_2$, *Nat. Commun.* **11**, 3985 (2019).

- [123] L. Muechler, E. Liu, J. Gayles, Q. Xu, C. Felser, and Y. Sun, Emerging chiral edge states from the confinement of a magnetic Weyl semimetal in $\text{Co}_3\text{Sn}_2\text{S}_2$, *Phys. Rev. B* **101**, 115106 (2020), arXiv:1712.08115.
- [124] D.-S. Ma, Y. Xu, C. S. Chiu, N. Regnault, A. A. Houck, Z. Song, and B. A. Bernevig, Spin-orbit-induced topological flat bands in line and split graphs of bipartite lattices *Phys. Rev. Lett.* **125**, 266403 (2020), arXiv:2008.08231.
- [125] J. X. Yin, S. S. Zhang, G. Chang, Q. Wang, S. S. Tsirkin, Z. Guguchia, B. Lian, H. Zhou, K. Jiang, I. Belopolski, N. Shumiya, D. Multer, M. Litskevich, T. A. Cochran, H. Lin, Z. Wang, T. Neupert, S. Jia, H. Lei, and M. Z. Hasan, Negative flat band magnetism in a spin-orbit-coupled correlated kagome magnet, *Nature Physics* **15**, 443 (2019).
- [126] G. Li, Q. Xu, W. Shi, C. Fu, L. Jiao, M. E. Kamminga, M. Yu, H. Tüysüz, N. Kumar, V. Süß, R. Saha, A. K. Srivastava, S. Wirth, G. Auffermann, J. Gooth, S. Parkin, Y. Sun, E. Liu, and C. Felser, Surface states in bulk single crystal of topological semimetal $\text{Co}_3\text{Sn}_2\text{S}_2$ toward water oxidation, *Science Advances* **5**, eaaw9867 (2019).
- [127] Q. Wang, Y. Xu, R. Lou, Z. Liu, M. Li, Y. Huang, D. Shen, H. Weng, S. Wang, and H. Lei, Large intrinsic anomalous Hall effect in half-metallic ferromagnet $\text{Co}_3\text{Sn}_2\text{S}_2$ with magnetic Weyl fermions, *Nature Communications* **9**, 3681 (2018).
- [128] S. Nie, G. Xu, F. B. Prinz, and S.-C. Zhang, Topological semimetal in honeycomb lattice LnSI, *Proceedings of the National Academy of Sciences* **114**, 10596 (2017).
- [129] M. Kang, L. Ye, S. Fang, J.-S. You, A. Levitan, M. Han, I. Facio, C. Jozwiak, A. Bostwick, E. Rotenberg, M. K. Chan, R. D. McDonald, D. Graf, K. Kaznatcheev, E. Vescovo, D. C. Bell, E. Kaxiras, J. Van den Brink, M. Richter, M. Prasad Ghimire, J. G. Checkelsky, and R. Comin, Dirac fermions and flat bands in the ideal kagome metal FeSn, *NATURE MATERIALS* **19**, 163 (2020).

- [130] L. Ye, M. Kang, J. Liu, F. Von Cube, C. R. Wicker, T. Suzuki, C. Jozwiak, A. Bostwick, E. Rotenberg, D. C. Bell, L. Fu, R. Comin, and J. G. Checkelsky, Massive Dirac fermions in a ferromagnetic kagome metal, *Nature* **555**, 638 (2018), arXiv:1709.10007.

The paper reports about surface and bulk Dirac fermions as well as flat bands in the antiferromagnetic Kagome metal FeSn.

- [131] S. Nakatsuji, N. Kiyohara, and T. Higo, Large anomalous Hall effect in a non-collinear antiferromagnet at room temperature, *NATURE* **527**, 212 (2015).

First report of a large anomalous Hall effect in an antiferromagnet Mn₃Sn with vanishingly small magnetization.

- [132] A. K. Nayak, J. E. Fischer, Y. Sun, B. Yan, J. Karel, A. C. Komarek, C. Shekhar, N. Kumar, W. Schnelle, J. Kuebler, C. Felser, and S. S. P. Parkin, Large anomalous Hall effect driven by a nonvanishing Berry curvature in the noncollinear antiferromagnet Mn₃Ge, *SCIENCE ADVANCES* **2**, e1501870 (2016).

- [133] Z. Liu, M. Li, Q. Wang, G. Wang, C. Wen, K. Jiang, X. Lu, S. Yan, Y. Huang, D. Shen, J.-X. Yin, Z. Wang, Z. Yin, H. Lei, and S. Wang, Orbital-selective Dirac fermions and extremely flat bands in frustrated kagome-lattice metal CoSn, *Nat Commun* **11**, 4002 (2020).

- [134] J.-X. Yin, W. Ma, T. A. Cochran, X. Xu, S. S. Zhang, H.-J. Tien, N. Shumiya, G. Cheng, K. Jiang, B. Lian, Z. Song, G. Chang, I. Belopolski, D. Multer, M. Litskevich, Z.-J. Cheng, X. P. Yang, B. Swidler, H. Zhou, H. Lin, T. Neupert, Z. Wang, N. Yao, T.-R. Chang, S. Jia, and M. Z. Hasan, Quantum-limit Chern topological magnetism in TbMn₆Sn₆, *Nature* **583**, 533 (2020).

A topological Kagome magnet with strong out-of-plane magnetization realized in TbMn₆Sn₆ and identified by scanning tunnelling microscopy.

- [135] T. Asaba, S. M. Thomas, M. Curtis, J. D. Thompson, E. D. Bauer, and F. Ronning, Anomalous Hall effect in the kagome ferrimagnet GdMn_6Sn_6 , *Phys. Rev. B* **101**, 174415 (2020).
- [136] W. Ma, X. Xu, J.-X. Yin, H. Yang, H. Zhou, Z.-J. Cheng, Y. Huang, Z. Qu, F. Wang, M. Z. Hasan, and S. Jia, Rare Earth Engineering in $R\text{-Mn}_6\text{Sn}_6$ ($R = \text{Gd-Tm, Lu}$) Topological Kagome Magnets, *Phys. Rev. Lett.* **126**, 246602 (2021).
- [137] J.-X. Yin, S. S. Zhang, H. Li, K. Jiang, G. Chang, B. Zhang, B. Lian, C. Xiang, I. Belopolski, H. Zheng, T. A. Cochran, S.-Y. Xu, G. Bian, K. Liu, T.-R. Chang, H. Lin, Z.-Y. Lu, Z. Wang, S. Jia, W. Wang, and M. Z. Hasan, Giant and anisotropic spin-orbit tunability in a strongly correlated kagome magnet, *Nature* **562**, 91 (2018).
- [138] Z. Wang, M. G. Vergniory, S. Kushwaha, M. Hirschberger, E. V. Chulkov, A. Ernst, N. P. Ong, R. J. Cava, and B. A. Bernevig, Time-reversalbreaking Weyl fermions in magnetic Heusler alloys, *Phys. Rev. Lett.* **117**, 236401 (2016).

This paper reports about the first prediction of ferromagnetic Weyl semimetal

- [139] J. Kübler and C. Felser, Weyl points in the ferromagnetic Heusler compound Co_2MnAl , *EPL (Europhysics Letters)* **114**, 47005 (2016).
- [140] T. Graf, C. Felser, and S. S. P. Parkin, Simple rules for the understanding of Heusler compounds, *PROGRESS IN SOLID STATE CHEMISTRY* **39**, 1 (2011).

This article summarizes the wide range of properties in the family of Heusler compounds

- [141] P. Li, J. Koo, W. Ning, J. Li, L. Miao, L. Min, Y. Zhu, Y. Wang, N. Alem, C.-X. Liu, Z. Mao, and B. Yan, Giant room temperature anomalous Hall effect and tunable topology in a ferromagnetic topological semimetal Co_2MnAl , *NATURE COMMUNICATIONS* **11**, 3476 (2020).
- [142] K. Manna, Y. Sun, L. Muechler, J. Kübler, and C. Felser, Heusler, Weyl and Berry, *Nature Reviews Materials* **3**, 244 (2018).

- [143] S. N. Guin, K. Manna, J. Noky, S. J. Watzman, C. Fu, N. Kumar, W. Schnelle, C. Shekhar, Y. Sun, J. Gooth, and C. Felser, Anomalous Nernst effect beyond the magnetization scaling relation in the ferromagnetic Heusler compound Co_2MnGa , *NPG Asia Materials* **11**, 16 (2019).
- [144] K. Manna, L. Muechler, T.-H. Kao, R. Stinshoff, Y. Zhang, J. Gooth, N. Kumar, G. Kreiner, K. Koepernik, R. Car, J. Kuebler, G. H. Fecher, C. Shekhar, Y. Sun, and C. Felser, From colossal to zero: Controlling the anomalous Hall effect in magnetic Heusler compounds via Berry curvature design, *PHYSICAL REVIEW X* **8**, 041045 (2018).
- [145] A. Sakai, S. Minami, T. Koretsune, T. Chen, T. Higo, Y. Wang, T. Nomoto, M. Hirayama, S. Miwa, D. NishioHamane, F. Ishii, R. Arita, and S. Nakatsuji, Iron-based binary ferromagnets for transverse thermoelectric conversion, *NATURE* **581**, 53 (2020).
- [146] M. Hirschberger, S. Kushwaha, Z. Wang, Q. Gibson, S. Liang, C. A. Belvin, B. A. Bernevig, R. J. Cava, and N. P. Ong, The chiral anomaly and thermopower of Weyl fermions in the half-Heusler GdPtBi , *Nature Materials* **15**, 1161 (2016).
- [147] S. Liang, J. Lin, S. Kushwaha, J. Xing, N. Ni, R. J. Cava, and N. P. Ong, Experimental tests of the chiral anomaly magnetoresistance in the Dirac-Weyl semimetals Na_3Bi and GdPtBi , *Phys. Rev. X* **8**, 031002 (2018).
- [148] C. Shekhar, N. Kumar, V. Grinenko, S. Singh, R. Sarkar, H. Luetkens, S.-C. Wu, Y. Zhang, A. C. Komarek, E. Kampert, Y. Skourski, J. Wosnitza, W. Schnelle, A. McCollam, U. Zeitler, J. Kübler, B. Yan, H.-H. Klauss, S. S. P. Parkin, and C. Felser, Anomalous Hall effect in Weyl semimetal half-Heusler compounds $RPtBi$ ($R = \text{Gd}$ and Nd), *Proceedings of the National Academy of Sciences* **115**, 9140 (2018).
- [149] N. Kumar, S. N. Guin, C. Felser, and C. Shekhar, Planar Hall effect in the Weyl semimetal GdPtBi , *Physical Review B* **98**, 041103 (2018).

- [150] C. Schindler, S. Galeski, W. Schnelle, R. Wawrzynczak, W. Abdel-Haq, S. N. Guin, J. Kroder, N. Kumar, C. Fu, H. Borrmann, C. Shekhar, C. Felser, T. Meng, A. G. Grushin, Y. Zhang, Y. Sun, and J. Gooth, Anisotropic electrical and thermal magnetotransport in the magnetic semimetal GdPtBi, **PHYSICAL REVIEW B** **101**, 125119 (2020).
- [151] J. Yu, B. Yan, and C.-X. Liu, Model Hamiltonian and time reversal breaking topological phases of antiferromagnetic half-Heusler materials, **PHYSICAL REVIEW B** **95**, 235158 (2017).
- [152] K. Kuroda, T. Tomita, M. T. Suzuki, C. Bareille, A. A. Nugroho, P. Goswami, M. Ochi, M. Ikhlas, M. Nakayama, S. Akebi, R. Noguchi, R. Ishii, N. Inami, K. Ono, H. Kumigashira, A. Varykhalov, T. Muro, T. Koretsune, R. Arita, S. Shin, T. Kondo, and S. Nakatsuji, Evidence for magnetic Weyl fermions in a correlated metal, **NATURE MATERIALS** **16**, 1090 (2017).
- [153] M. Ikhlas, T. Tomita, T. Koretsune, M.-T. Suzuki, D. Nishio-Hamane, R. Arita, Y. Otani, and S. Nakatsuji, Large anomalous Nernst effect at room temperature in a chiral antiferromagnet, **Nature Physics** **13**, 1085 (2017).
- [154] T. Higo, H. Man, D. B. Gopman, L. Wu, T. Koretsune, O. M. J. van't Erve, Y. P. Kabanov, D. Rees, Y. Li, M.-T. Suzuki, S. Patankar, M. Ikhlas, C. L. Chien, R. Arita, R. D. Shull, J. Orenstein, and S. Nakatsuji, Large magneto-optical Kerr effect and imaging of magnetic octupole domains in an antiferromagnetic metal, **NATURE PHOTONICS** **12**, 73 (2018).
- [155] L. Smejkal, Y. Mokrousov, B. Yan, and A. H. Mac-Donald, Topological antiferromagnetic spintronics, **NATURE PHYSICS** **14**, 242 (2018).
- [156] T. Suzuki, L. Savary, J.-P. Liu, J. W. Lynn, L. Balents, and J. G. Checkelsky, Singular angular magnetoresistance in a magnetic nodal semimetal, **Science** **365**, 377 (2019).
- [157] P. Puphal, V. Pomjakushin, N. Kanazawa, V. Ukleev, D. J. Gawryluk, J. Ma, M. Naamneh, N. C. Plumb, L. Keller, R. Cubitt, E. Pomjakushina, and J. S. White,

Topological magnetic phase in the candidate Weyl semimetal CeAlGe, *Phys. Rev. Lett.* **124**, 017202 (2020).

- [158] D. S. Sanchez, G. Chang, I. Belopolski, H. Lu, J.-X. Yin, N. Alidoust, X. Xu, T. A. Cochran, X. Zhang, Y. Bian, S. S. Zhang, Y.-Y. Liu, J. Ma, G. Bian, H. Lin, S.-Y. Xu, S. Jia, and M. Z. Hasan, Observation of Weyl fermions in a magnetic non-centrosymmetric crystal, *Nat. Commun.* **11**, 3356 (2020).
- [159] S.-Y. Xu, N. Alidoust, G. Chang, H. Lu, B. Singh, I. Belopolski, D. Sanchez, X. Zhang, G. Bian, H. Zheng, M.A. Husanu, Y. Bian, S.-M. Huang, C.-H. Hsu, T.-R. Chang, H.-T. Jeng, A. Bansil, V. N. Strocov, H. Lin, S. Jia, and M. Z. Hasan, Discovery of Lorentz-violating type II Weyl fermions in LaAlGe, *Sci. Adv.* **3**, e1603266 (2017).
- [160] H. Guo, C. Ritter, and A. C. Komarek, Direct determination of the spin structure of $\text{Nd}_2\text{Ir}_2\text{O}_7$ by means of neutron diffraction, *Physical Review B* **94**, 161102 (2016).
- [161] P. Goswami, B. Roy, and S. Das Sarma, Competing orders and topology in the global phase diagram of pyrochlore iridates, *Physical Review B* **95**, (2017), arXiv:1603.02273.
- [162] K. Ueda, T. Oh, B. J. Yang, R. Kaneko, J. Fujioka, N. Nagaosa, and Y. Tokura, Magnetic-field induced multiple topological phases in pyrochlore iridates with Mott criticality, *Nature Communications* **8**, 15515 (2017).
- [163] L. Savary, E. G. Moon, and L. Balents, New type of quantum criticality in the pyrochlore iridates, *Physical Review X* **4**, 041027 (2014), arXiv:1403.5255.
- [164] K. Matsuhira, M. Wakushima, R. Nakanishi, T. Yamada, A. Nakamura, W. Kawano, S. Takagi, and Y. Hinatsu, Metal-insulator transition in pyrochlore iridates $\text{Ln}_2\text{Ir}_2\text{O}_7$ ($\text{Ln} = \text{Nd, Sm, and Eu}$), *Journal of the Physical Society of Japan* **76**, 043706 (2007).
- [165] M. Nakayama, T. Kondo, Z. Tian, J. Ishikawa, M. Halim, C. Bareille, W. Malaeb, K. Kuroda, T. Tomita, S. Ideta, K. Tanaka, M. Matsunami, S. Kimura, N. Inami, K. Ono, H. Kumigashira, L. Balents, S. Nakatsuji, and S. Shin, Slater to Mott Crossover in the Metal to Insulator Transition of $\text{Nd}_2\text{Ir}_2\text{O}_7$, *Phys. Rev. Lett.* **117**, 056403 (2016).

- [166] Z. Tian, Y. Kohama, T. Tomita, H. Ishizuka, T. H. Hsieh, J. J. Ishikawa, K. Kindo, L. Balents, and S. Nakatsuji, Field-induced quantum metal–insulator transition in the pyrochlore iridate $\text{Nd}_2\text{Ir}_2\text{O}_7$, *Nat. Phys.* **12**, 134 (2016).
- [167] E. Y. Ma, Y. T. Cui, K. Ueda, S. Tang, K. Chen, N. Tamura, P. M. Wu, J. Fujioka, Y. Tokura, and Z. X. Shen, Mobile metallic domain walls in an all-in-all-out magnetic insulator, *Science* **350**, 538 (2015).
- [168] Y. Yamaji and M. Imada, Metallic interface emerging at magnetic domain wall of antiferromagnetic insulator: Fate of extinct Weyl electrons, *Physical Review X* **4**, 021035 (2014), arXiv:1306.2022.
- [169] T. Suzuki, R. Chisnell, A. Devarakonda, Y.-T. Liu, W. Feng, D. Xiao, J. W. Lynn, and J. G. Checkelsky, Large anomalous Hall effect in a half-Heusler antiferromagnet, *Nature Physics* **12**, 1119 (2016).
- [170] E. Vilanova Vidal, G. Stryganyuk, H. Schneider, C. Felser, and G. Jakob, Exploring Co_2MnAl Heusler compound for anomalous Hall effect sensors, *Applied Physics Letters - APPL PHYS LETT* **99**, 132509 (2011).
- [171] C. Wuttke, F. Caglieris, S. Sykora, F. Scaravaggi, A. A. U. B. Wolter, K. Manna, V. Suess, C. Shekhar, C. Felser, B. Buechner, and C. Hess, Berry curvature unravelled by the anomalous Nernst effect in Mn_3Ge , *PHYSICAL REVIEW B* **100**, 085111 (2019).
- [172] J. Li, Y. Li, S. Du, Z. Wang, B. L. Gu, S. C. Zhang, K. He, W. Duan, and Y. Xu, Intrinsic magnetic topological insulators in van der Waals layered MnBi_2Te_4 family materials, *Science Advances* **5**, eaaw5685 (2019), arXiv:1808.08608.
- [173] Z. Song, T. Zhang, Z. Fang, and C. Fang, Quantitative mappings between symmetry and topology in solids, *Nature Communications* **9**, 3530 (2018).
- [174] Z.-D. Song, L. Elcoro, Y.-F. Xu, N. Regnault, and B. A. Bernevig, Fragile phases as affine monoids: Classification and material examples, *Phys. Rev. X* **10**, 031001 (2020).

- [175] Z.-D. Song, L. Elcoro, and B. A. Bernevig, Twisted bulk-boundary correspondence of fragile topology, *Science* **367**, 794 (2020).
- [176] B. Bradlyn, L. Elcoro, J. Cano, M. G. Vergniory, Z. Wang, C. Felser, M. I. Aroyo, and B. A. Bernevig, Topological quantum chemistry, *Nature* **547**, 298 (2017).
- [177] M. G. Vergniory, L. Elcoro, Z. Wang, J. Cano, C. Felser, M. I. Aroyo, B. A. Bernevig, and B. Bradlyn, Graph theory data for topological quantum chemistry, *Phys. Rev. E* **96**, 023310 (2017).
- [178] B. Bradlyn, Z. Wang, J. Cano, and B. A. Bernevig, Disconnected elementary band representations, fragile topology, and wilson loops as topological indices: An example on the triangular lattice, *Phys. Rev. B* **99**, 045140 (2019).
- [179] J. Kruthoff, J. de Boer, J. van Wezel, C. L. Kane, and R.-J. Slager, Topological classification of crystalline insulators through band structure combinatorics, *Phys. Rev. X* **7**, 041069 (2017).
- [180] E. Khalaf, H. C. Po, A. Vishwanath, and H. Watanabe, Symmetry indicators and anomalous surface states of topological crystalline insulators, *Phys. Rev. X* **8**, 031070 (2018).
- [181] M. Kenzelmann, A. B. Harris, S. Jonas, C. Broholm, Schefer, S. B. Kim, C. L. Zhang, S.-W. Cheong,O. P. Vajk, and J. W. Lynn, Magnetic inversion symmetry breaking and ferroelectricity in tbmno₃, *Phys. Rev. Lett.* **95**, 087206 (2005).
- [182] S. V. Gallego, J. M. Perez-Mato, L. Elcoro, E. S. Tasci, R. M. Hanson, K. Momma, M. I. Aroyo, and G. Madariaga, MAGNDATA: towards a database of magnetic structures. I. The commensurate case, *Journal of Applied Crystallography* **49**, 1750 (2016).
- [183] I. Belopolski, K. Manna, D. S. Sanchez, G. Chang, B. Ernst, J. Yin, S. S. Zhang, T. Cochran, N. Shumiya, H. Zheng, B. Singh, G. Bian, D. Multer, M. Litskevich, X. Zhou, S. M. Huang, B. Wang, T. R. Chang, S. Y. Xu, A. Bansil, C. Felser, H. Lin, and M.

Zahid Hasan, Discovery of topological Weyl fermion lines and drumhead surface states in a room temperature magnet, **Science 365**, 1278 (2019).

This is the first proof of a ferromagnetic nodal line half metal with surface states that take the form of drumheads via ARPES in Co₂MnGa.

Figures

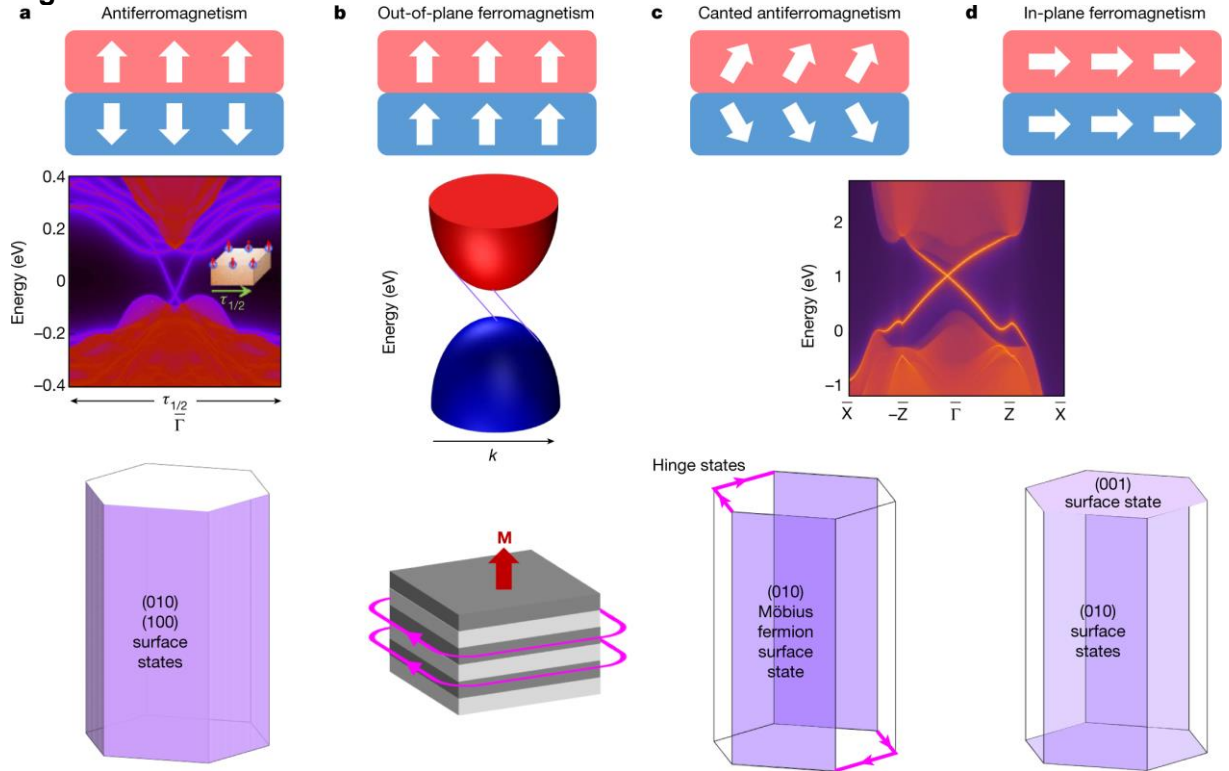


FIG. 1. **Interplay between magnetic orders and topology.** Depending on the spin

configuration, the $\text{MnBi}_{2n}\text{Te}_{3n+1}$ system is predicted to be (a) an AFMTI - with a single gapless Dirac cone protected by $\{\text{T}|00\frac{1}{2}\}$ on the symmetry-preserving (010) (or (100) surface), while the symmetry non-preserving (001) surface is gapped, (b) in a thin 2D sample with only a few layers, a QAHE state with $C = 1$ (AXI) or $C = 2$ depending on the number of layers and with Chiral edge states (c) a Möbius Insulator in canted AFM which respects glide mirror $\{M_x|00\frac{1}{2}\}$ symmetry with M_x mirror followed by half lattice translation. The insulator shows surface states on the symmetry preserving (010) surface but not on the (100) and (001). Two opposite (010) surfaces are linked together by 1D chiral hinge states, manifesting the higher-order nature (HOTI) of the system. The surface state is a Dirac cone, whose position is on the $\bar{\Gamma}-\bar{Z}$ line, and their mirror eigenvalues, proportional to $e^{ikz/2}$ require two BZ (4π) to return to themselves, hence the Möbius name. (d) a TCI phase for in-plane FM, where the glide mirror $\{M_x|00\frac{1}{2}\}$ is promoted to a mirror M_x , and now a surface state appears on both symmetry preserving (010) and hte (001) surfaces.

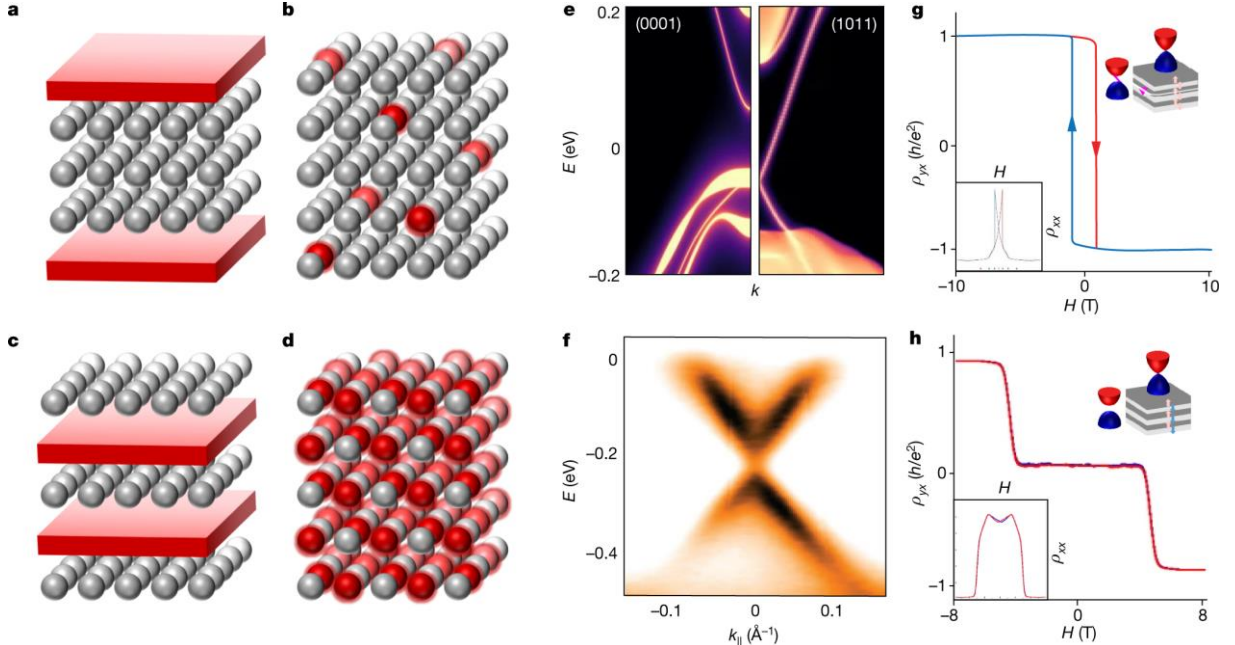


FIG. 2. Magnetic topological insulators - Realizations and MnBi_2Te_4 case study. There are four main approaches for realizing a magnetic TI: (a) Deposition of a magnetic layer over a TI surface (eg $\text{EuS}/\text{Bi}_2\text{Se}_3$). (b) Magnetic element doping of a TI (e.g. $\text{Bi}_{2-x}\text{Cr}_x\text{Te}_3$). (c) Stoichiometrically interleaved magnetic layers within the TI unit cell (e.g. MnBi_2Te_4). (d) Intrinsically stoichiometric magnetic TIs (e.g. EuCd_2As_2). The AFM TI MnBi_2Te_4 was recently shown to exhibit quantized anomalous Hall conductance in the thin film limit with an exciting dependence on parity of layer number (e) ab initio calculation of its surface band structure predicts presence of Dirac states on surfaces that preserve combined time reversal and half unit cell translation operation and massive ones on those that break it (right and left panels, respectively) [28]. (f) spectroscopic ARPES measurement images Dirac surface states with possible induced gap at the Dirac node [10]. The magneto-transport responses show prominent magnetic topological response (g) For even septuple-layer thin film QAHE is observed with quantized Hall resistance [15] (h) while for odd septuple-layer axion response is found with null Hall response [78].

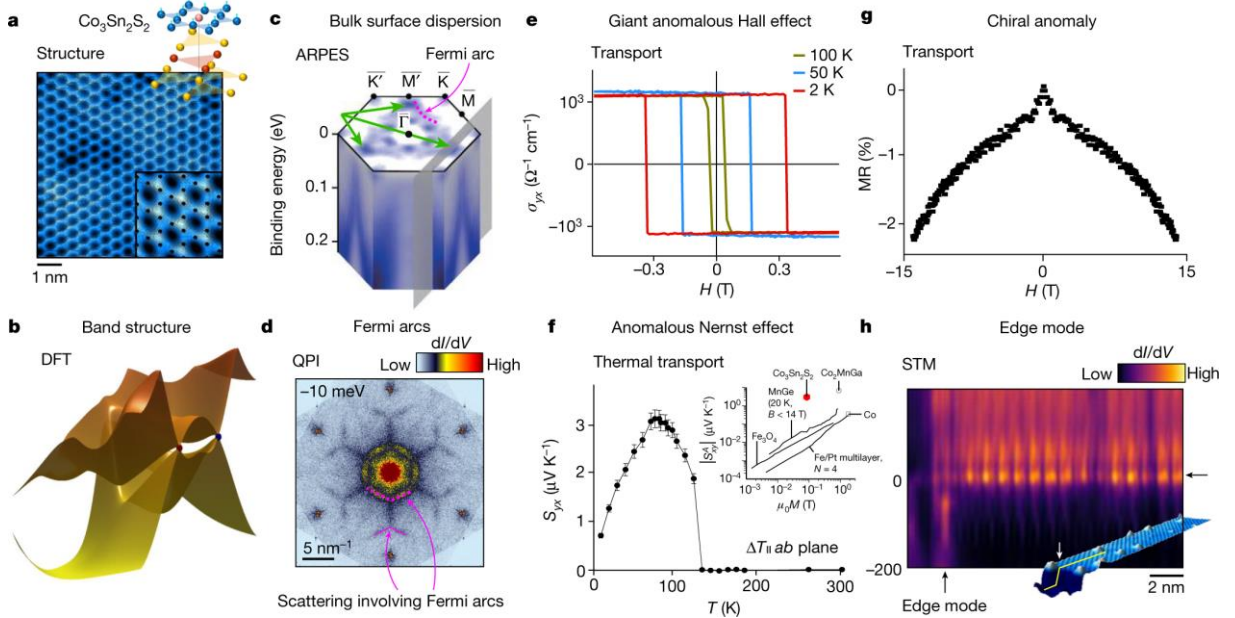
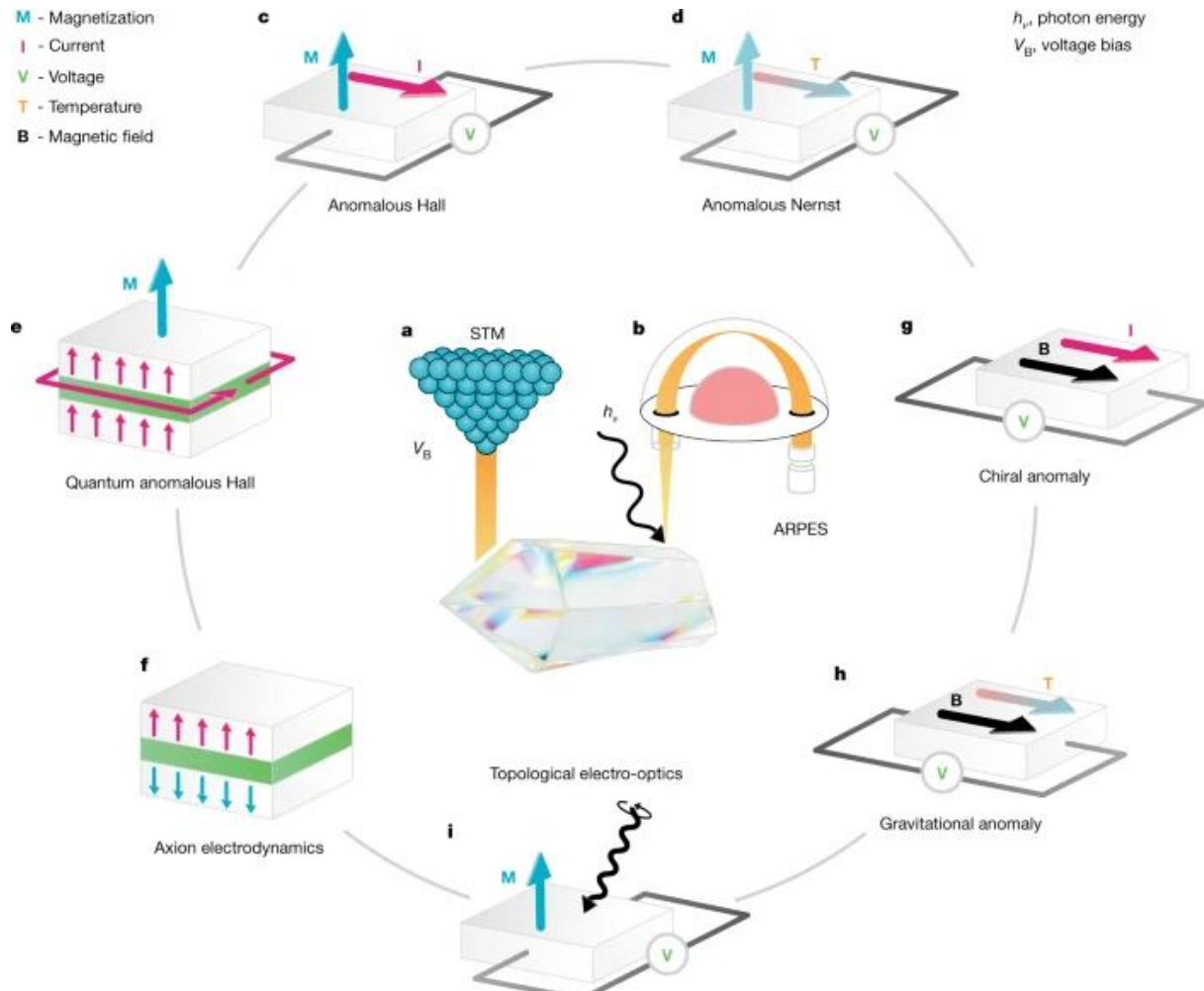


FIG. 3. Magnetic Topological semimetals - $\text{Co}_2\text{Sn}_2\text{S}_2$ case study The ferromagnetic WSM $\text{Co}_2\text{Sn}_2\text{S}_2$ exhibits many of the phenomena associated with magnetic topological matter (see Box 2) (a) Atomic structure contains Kagome layers of Co magnetic ions (inset) seen in STM topography [9]. (b) ab initio calculation of its band structure within the FM phase finds 6 bulk Weyl nodes with Dirac-like dispersion. (c) The bulk Weyl bands and corresponding surface Fermi arc states (magenta) are captured in ARPES [118] (d) Scattering processes involving Fermi arc states are also imaged in STM through QPI (magenta) [9]. (e) Transverse magnetotransport ($B \perp I$) finds a giant AHE [119] (f) as well as large anomalous Nernst signal ($B \perp \nabla T$) that onsets with finite coercive field within the FM phase [120]. (g) Strong negative magneto resistance ($B \parallel I$) is further detected possibly signifying chiral anomaly [119]. (h) STM spectroscopic imaging finds an increased density of states (marked by open arrow) localized next to crystallographic step edge (topography in inset) attributed to edge mode [121]. Zero-bias conductance peak (marked by solid arrow) possibly originates from geometric frustration due to Kagome structure [122]

BOX 1. Prediction of magnetic topological materials. WaveFunction Representations.

The framework for classifying and analyzing magnetic crystals and their topology is that of the 1651 magnetic symmetry groups (MSGs). A complete catalogue of MSGs and their topological phases is now available, for the first time, on the [Bilbao Crystallographic Server \(BCS\)](#). The steps for high-throughput material discovery are: First, an ab-initio calculation obtains the electronic wavefunction representations (called “symmetry data”) at high symmetry points for a specific material. Efficient M/TQC [176–178] and related methods [40, 173, 179, 180] require only the electronic wavefunctions at a small number of specific, high-symmetry momenta. **Topological Indices.** Second, the symmetry data is used to compute the topological indices of a set of bands. The computation background is rather complicated and tedious for a large number of bands; publicly available codes ([Check Magnetic Topology](#)) can now automate this process. Given the information available in the band’s symmetry data, the code checks both whether a set of bands in the Brillouin zone can form an insulator. If not, they are a TSM. If yes, the code further checks whether the insulator can be expressed as a sum of atomic, trivial insulators. If not, it is topological. Further division of topological class is performed and materials are tabulated in a way similar to the spirit of a “periodic table” of compounds. **Material Prediction.** Band structures and topological phase diagrams depending on Hubbard U interaction are computed and posted in [Topological Materials Database](#). Despite the results of [6–8], and the recent experimental identification of novel magnetic TIs [10, 16] and TSMs [9, 111, 118], the low number of materials with magnetic structures measured through neutron diffraction and matched with magnetic SGs hinders magnetic material discovery. Neutron scattering measurements [181] for every magnetic compound, coupled with theoretical analysis of the spin wave spectrum are needed to determine the MSG. Fortunately, the list of compounds for which the MSG is determined by the [MAGNDATA](#) application on the BCS [182] is growing daily, from 500 a year ago [6] to 1000 today. Knowing the MSG allows for far more accurate ab-initio calculations of the band

structure, which can then be used [7] to determine the topological classification of the magnetic materials.



BOX 2. Experimental identification of magnetic topological materials

Band structure mapping: a) Scanning tunneling microscopy (STM) and b) Angle-resolved Photoemission Spectroscopy (ARPES) probe spectroscopic topological fingerprints mainly through the concept of bulk-boundary correspondence of the electronic band structure. Magnetic Weyl and Dirac semimetals exhibit linear dispersion in the bulk and Fermi arcs at their surfaces, whereas nodal line semimetals host complex drum head surface states [9, 111, 118, 183]. In magnetic TIs the main spectroscopic challenge is to image the gapped surface states [27, 28].

Transport and optical properties: Magnetic topological materials that host an enhanced Berry curvature further exhibit extreme responses to external stimuli such as magnetic field, voltage or current bias, temperature gradient and optical excitation that can be applied in various longitudinal and transverse combinations as shown in c) to i) [102, 119, 120, 143, 153]. c) For observing the anomalous Hall effect, an electric current is injected normal to the

magnetization. The resulting Hall resistivity of a ferro- or ferrimagnetic compound is then proportional to the magnetization and enhanced close to Dirac and Weyl points or nodal lines [94] d) Analogous to the AHE, an ANE is observed in measurements of heat current, where a transverse voltage is produced by a temperature gradient and the magnetization orthogonal to each other. e) In extreme cases the anomalous Hall response becomes quantized [27] f). Whenever the magnetization on opposite boundaries has opposite polarity an Axion insulator is formed in which the electrons exhibit axion electrodynamics. g) The chiral anomaly in topological materials is manifested by a negative magneto-resistance in response to parallel electric current and magnetic field. The negative magneto resistance arises from the magnetic-field-induced imbalance in the number of fermions in each pair of Weyl nodes with opposite chirality. h) The same experimental setup with a thermal gradient instead of an electric field, probes the gravitational anomaly. I) Nonlinear optical conductivity components should be enhanced due to the large Berry in semimetal and nodal line compounds.

TABLE I. Synthesis-methods, Anomalous transport properties of magnetic topological semimetals.

Compound	Synthesis	Topology type	Magnetism	T _C or T _N (K)	AHC ($\sim 2\text{K}$) ($\Omega^{-1} \text{cm}^{-1}$)	ANE ($\mu\text{V K}^{-1}$)	Ref.
GdPtBi	Flux	Weyl	AFM	9	200	–	[169]
Co ₂ MnGa	Bridgeman	Nodal line	FM	686	1600	6 (300 K)	[102, 143, 144]
Co ₂ MnAl	Floating-zone	Nodal line	FM	726	2000	–	[141, 170]
Co ₃ Sn ₂ S ₂	Flux, CVD	Weyl	FM, non-collinear	177	1130	3 (80 K)	[119, 120]
FeSn	Flux	Dirac	AFM	365	–	–	[129]
Fe ₃ Sn ₂	CVD	Dirac	FM	670	1050	–	[130]
Fe ₃ Ga	Czochralski	Nodal line	FM	720	610	6 (300 K)	[145]
Fe ₃ Al	Czochralski	Nodal line	FM	600	460	4 (300 K)	[145]
Fe ₃ GeTe ₂	CVD	Nodal line	FM	220	540 (10 K)	0.3 (50 K)	[122]
Mn ₃ Sn	Bridgeman, Czochralski	Weyl	AFM, non-collinear	100 (100 K)	0.6 (200 K)	–	[131, 153]
Mn ₃ Ge	Czochralski	Weyl	AFM, non-collinear	500	1.5 (100 K)	–	[132, 171]